journal of the mechanical behavior of biomedical materials 150 (2024) 106327

Contents lists available at ScienceDirect

Journal of the Mechanical Behavior of Biomedical Materials

journal homepage: www.elsevier.com/locate/jmbbm

On the thermal impact during drilling operations in guided dental surgery: An experimental and numerical investigation

Francesca Pupulin [a], Giorgio Oresta [a], Talha Sunar [b], Paolo Parenti [a,*]

[a] Department of Mechanical Engineering, Politecnico di Milano, via La Masa 1, 20156, Milan, Italy
[b] Department of Manufacturing Engineering, Karabuk University, 78050, Karabük, Turkey

ARTICLE INFO

Keywords:
Cutting temperature
Thermal field
Finite element modelling
Synthetic bone
Guided implantology
Thermal osteonecrosis

ABSTRACT

In recent years, a major development in dental implantology has been the introduction of patient-specific 3D-printed surgical guides. The utilization of dental guides offers advantages such as enhanced accuracy in locating the implant sites, greater simplicity, and reliability in performing bone drilling operations. However, it is important to note that the presence of such guides may contribute to a rise in cutting temperature, hence increasing the potential hazards of thermal injury to the patient's bone. The aim of this study is to examine the drilling temperature evolution in two distinct methods for 3D-printed surgical dental guides, one utilizing an internal metal bushing system and the other using external metal reducers. Cutting tests are done on synthetic polyurethane bone jaw models using a lab-scale automated Computer Numeric Control (CNC) machine to find out the temperature reached by different drilling techniques and compare them to traditional free cutting configurations. Thermal imaging and thermocouples, as well as the development of numerical simulations using finite element modeling, are used for the aim. The temperature of the tools' shanks experienced an average rise of 2.4 °C and 4.8 °C, but the tooltips exhibited an average increase of around 17 °C and 24 °C during traditional and guided dental surgery, respectively. This finding provides confirmation that both guided technologies have the capability to maintain temperatures below the critical limit for potential harm to bone and tissue. Numerical models were employed to validate and corroborate the findings, which exhibited identical outcomes when applied to genuine bone samples with distinct thermal characteristics.

1. Introduction

The evolution of modern dental implantology, diagnostic imaging techniques, more widely, the digital revolution led to the development of a new surgical protocol defined as computer-aided dental implantology or guided dental implantology. This new technique, which pivots on digital Additive Manufacturing, allows the positioning of the dental implant using a surgical guide (or template) whose design is patient specific. This technique enables the accurate implementation of the prosthetic project, thus enhancing the outcome of the surgeries.

Despite the enormous potential of this new technology, its widespread adoption in the dental industry is hindered by general clinical and economic concerns. One of the most important clinical considerations relates to the potential temperature increase caused by the presence of the surgical guide, which can increase the risk of thermal osteonecrosis (Timon and Keady, 2019), (Misir et al., 2009).

During implant site preparation, a temperature increment in the tissue surrounding the implant site is always generated. Overheating could cause necrosis, fibrosis, caustic bone degeneration, and usually decreased osteoblastic activity (Scarano et al., 2020) and the increase temperature impact caused by the adoption of the guiding procedure can be detrimental.

Some possible sources can trigger this temperature increase when guided surgery is adopted. On one side, the guide can prevent the proper flushing of the cutting zone with the refrigerant fluid, thus reducing the chip evacuation and inducing heat accumulation. At the same time, when placed on the bone, it can also increase the tool shank temperature due to the friction generated in the tool-guide contact zone. Furthermore, it might act as additional shielding, impeding the proper heat diffusion, Fig. 1.

The investigation of temperature elevation is crucial, as it is closely connected with the dynamics of heat buildup, which in turn significantly influences the risks associated with damage to bone cells. At high temperatures bone cells (osteoblasts and osteoclasts) die, so bone no longer

* Corresponding author.
E-mail address: paolo.parenti@polimi.it (P. Parenti).

https://doi.org/10.1016/j.jmbbm.2023.106327
Received 30 October 2023; Received in revised form 10 December 2023; Accepted 11 December 2023
Available online 13 December 2023

grows and osseointegration of the implant is never achieved (so it will fail). All this would make the custom guide design futile.

Nevertheless, given the emerging nature of this innovative technology, it is vital for both industry stakeholders and the scientific community to address these concerns.

The main purpose of this study is to examine, both experimentally and numerically, the cutting temperature generation by adopting two different types of 3D printed surgical dental guides. A general discussion about the thermal generation in guided dental surgery is presented, followed by a detailed description of the experimental method adopted for testing. After that, the collected temperature data are analyzed and discussed providing a qualitative comparison between the two guide methods. The Finite Element model for the evaluation of the temperature increase on biological bone is then introduced and its numerical results are discussed to compare the synthetic and biological bone materials thermal response.

1.1. State-of-the-Art on the thermal effects of guided surgery

As one of the main concerns in dental surgery, the temperature increase of the patient's bone is strictly related to the technology and tool geometry adopted (Bai et al., 2021) and (Ruga et al., 2017). Cutting with twist drills, nowadays is the most widely spread method for dental drilling thanks to its efficiency and cost-effectiveness. However, this method cannot guarantee the best accuracy and shows significant sensitivity to heat generation regarding cutting parameters, refrigeration, and tool wear (Lee et al., 2011). That is why customized surgical guides, associated to twist drill use, have been developed to allow the positioning of the implants at predetermined angles and depths in accordance with the patient's own diagnostic images. The use of guided surgery has several advantages, among which the most important is the reduction of the operating time and the minimization of the risk of injuries to critical structures but it can also show disadvantages related to increased pre-operative time and production costs (Tatakis et al., 2000). The dental guides are produced exploiting Additive Manufacturing, mainly by stereolithography (SLA) techniques (Chen et al., 2020), that permit using class I biocompatible resins, allowing autoclave sterilization (Türker et al., 2022). Misir et al. (2009) and Migliorati et al. (2013) studied the temperature increment during bone drilling by comparing guided and non-guided procedures. Even if they observed that guided surgery caused an increase in the temperature during the operation, they also found that the values reached never showed to be dangerous for the cell's survival. Instead, Stocchero et al. (2021) investigated the influence of 3D-printed surgical guides on the bovine bone's temperature, comparing four different cooling methods. They tested a supplementary internal irrigation system, the effect of only external irrigation, a system without irrigation, and an external irrigation system without using the guide. They concluded that there is always an increment in the temperature during drilling but that a nonrelevant difference exists between the four cooling methods. The same authors, in (Stocchero et al., 2019) carried out an in-vivo study on sheep that demonstrated that the proper selection of the drilling protocols is fundamental since it can affect the intraosseous temperature evolution not only during the drilling for site preparation but also during the implant's installation, with subsequent effects on the bone healing capacity. Frösch et al. (2019), compared the heat generation during guided and free drilling osteotomy approaches for different surgery protocols showing that statistically significant higher temperatures are generated in the guided method for all the drilling tools adopted. Waltenberger et al. (2022) examined the effect of different implant drilling template designs on heat generation during osteotomy. They reported that fully guided implant drilling templates reduced the cooling fluid at the osteotomy point. However, they noted that it is possible to moderate the temperature using fully guided templates with sufficient cooling water and adapted rotational speed. In their study, Choi et al. (2022) conducted a comparative analysis of heat generation during ex vivo implant preparation on bovine bone. The authors utilized several digital surgical guides, both with and without metallic sleeves/bushes, as well as different drilling bits, by finding that the presence of the guides produced a not significant increase of temperature of the cortical bone.

1.2. Thermal mechanisms in guided dental surgery

There are different phenomena involved in thermal generation during the dental drilling process, Fig. 2. First, the cutting process generates heat due to the bone removal operated by the rotational tool, and this heat evacuates through the removed chips and coolant, through the tool body itself, and lastly, through the patient tissues (bone and gum). The thermal problem in guided drilling may add thermal contributions. On one side, there is the contribution of the generated friction between the rotating tool and the fixed guide bushing. On the other, the guide can introduce some shielding effect of the refrigerant fluid that is delivered to the cutting zone then, causing a reduction of i) the flushing of the cutting zone (with decreased chip evacuation capacity and reduced fluid cooling effect), ii) the cutting lubrication (that leads to increased friction between the tool with the chip and the bone).

When fluid delivery is external, namely when the irrigation is embedded in the dental spindle and the refrigerant fluid falls from above, the accurate coupling between the guide and the tool shank together with the rotation of the helical tools prevent a proper flushing of the cutting zone.

The materials involved play an important role in the dissipation of the generated heat. While metals, typically adopted for the tools and the bushings (e.g., tool steel or stainless steel) are good conductors that

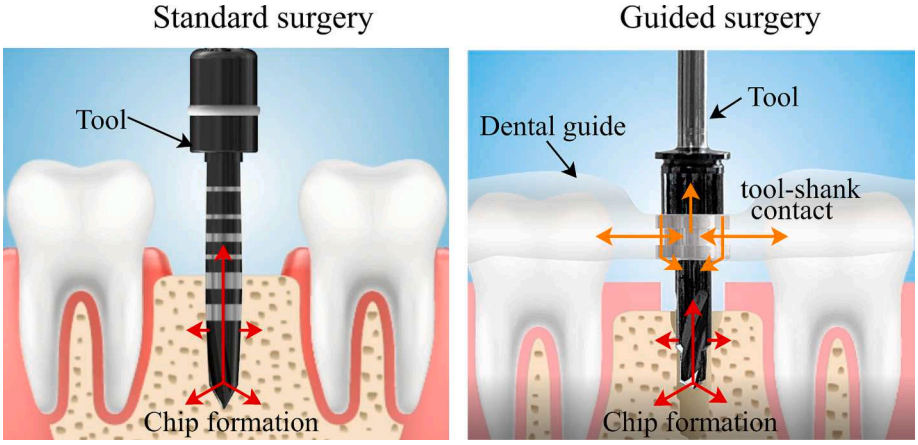

Fig. 1. Heat generation and transfer in standard and guided dental surgery.

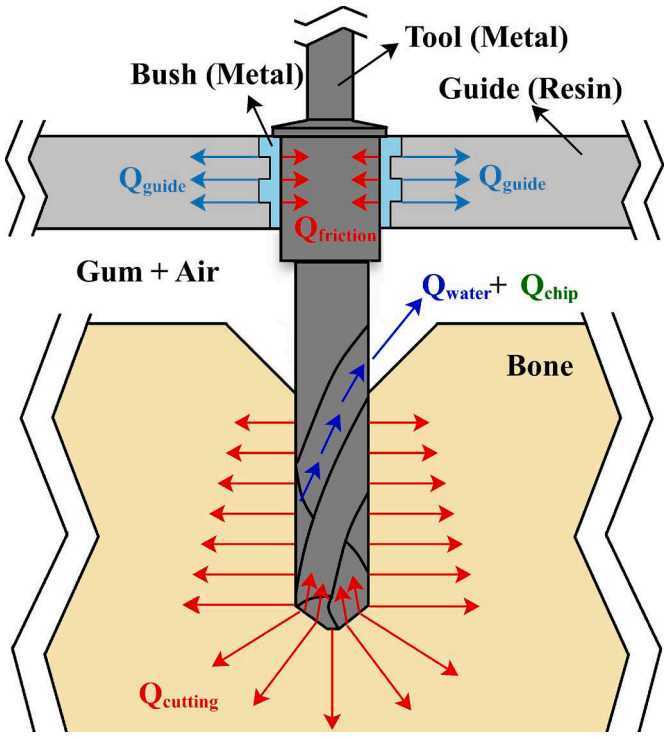

Fig. 2. Heat fluxes in the guided dental cutting.

support quick heat dissipation, the polymeric resin adopted for the guides behaves like an insulator, generating heat accumulation. Therefore, heat is transferred by conduction (with low resistance) along the drill bit, and then towards the guide and the bone, which are materials characterized by a higher thermal resistance.

The surgical operations' sequence and timing affect heat generation and accumulation. In fact, in dental surgery, multiple tools with increasing sizes (diameters and lengths) are adopted to obtain the final site dimension for the implant. This implies different heat generation for the different tools and certain cooling of the heated materials due to the idling times between the surgery steps, as shown in Fig. 3. When the bit is penetrating the bone, heat is generated and bone temperature rises, proportionally to the amount of removed chip volume and cutting efficiency. Therefore, different tools with variable diameters, cutting parameters and hole depth, generate different temperature rises. When the tool is removed from the bone for tool change, bone cools down proportionally to the tool change phase duration.

1.3. Aim of the work

This work studies the cutting temperature evolution of two distinct guided dental drilling systems and compares it with the free cutting configuration, performed without the guide. To attain a systematic and robust comparison, it was decided to opt for an in vitro testing utilizing synthetic bone made by medical grade polyurethane material (PU) and an automatic drilling system. Estimating the drilling temperature evolution when cutting genuine bone is in fact challenging for different reasons. On one side, natural bone structure is inhomogeneous and characterized by different densities (interindividual and intra-individual) which typically induce large cutting forces variability that can prevent a rigorous drilling systems comparison. Secondly, dental drilling is a manual surgery operation, therefore, implying the operator variability in the cutting process evolutional and control, especially of the axial drilling feed (and related force) that introduces a huge impact on cutting temperature evolution.

Among the sources of variability in the experimentation, the selected workpiece material represents one of the most critical aspects. Rigid polyurethane (PU) was adopted as a synthetic bone since it has the capacity to mimic both trabecular and cortical bones. This material is in fact produced by the polymerization reaction between isocyanate and hydroxyl groups and once polyurethane is created, it can be turned into foams or bulk resins by means of blowing agents. The reaction between water and isocyanate generates carbon dioxide, a gas that fills and expands the cells created during the mixing process, resulting in a closed solid cell structure. Although cancellous bone is characterized by an open porosity structure due to interconnecting rods and plates creating columns, the macro-structure is very similar to the closed foam structure of PU (Szivek et al., 1993). Since the foams can be tuned to obtain a stress-strain relationship close to the human bones, polyurethane foams are the gold standard among orthopedic materials for in vitro medical simulations (Calvert et al., 2010).

Polyurethane foams can vary a lot in their properties depending on their mixture (Thompson et al., 2003). This allows the creation of foams for an extensive range of applications, including biomedical ones ((ASTM F1839, 2014) defined the mechanical characteristics that a polyurethane foam must have to be used for testing orthopedic devices and instruments).

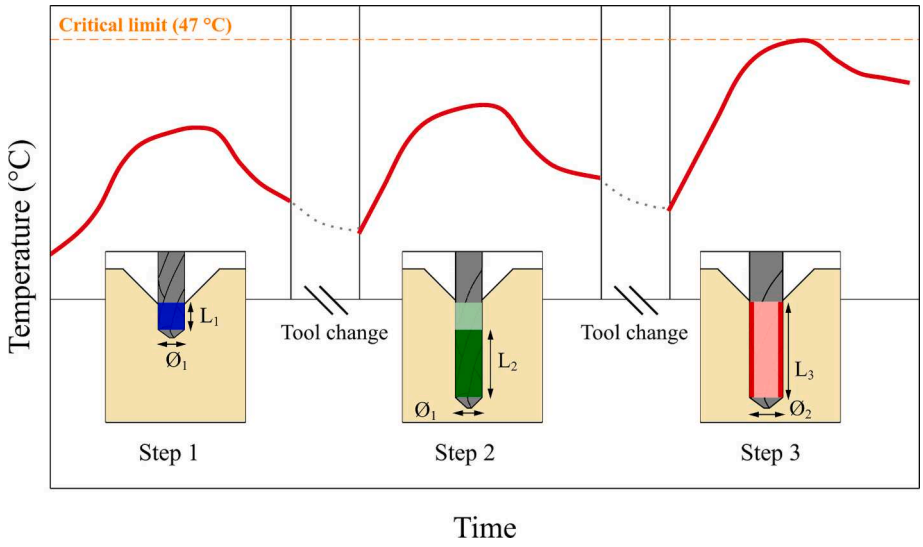

Fig. 3. A typical multi-step drilling cycle and (conceptual) cutting temperature evolution.

In this work, an indirect temperature evaluation on the tool during the in vitro testing is performed as a proxy of bone temperature evolution. This way is believed to bring to the best controllable experimental characterizations. In vivo temperature measurement in dental drilling would be in fact invasive, not easily implementable, and controllable.

During the tests, the temperatures are acquired in two different ways. The temperatures inside the polyurethane workpieces are measured by employing thermocouple sensors placed close to the drilled holes. On the other hand, indirect measurements of the tool temperature are performed via infrared imaging through an IR camera. These methods are the most adopted in literature to provide the bone temperature.

Thanks to the indirect measurement method, no contact between the sample and the sensor may affect the sample temperature itself. Moreover, it provides the temperature distribution along the whole surface and not only locally at the contact point. In literature, these devices are used following two main possibilities: measuring the temperature of a surface that is placed at a certain distance from the drilling site or, in a second way, measuring the tool temperature during drilling as Sugita et al. (2009) made, or immediately after the process (Fernandes et al., 2016). Regarding the first method, the drilling site distance varied from 0.5 mm to 3 mm, while the distance from the surface to the IR camera objective ranged from 500 mm to 1000 mm.

In the present work, the drill bit is measured during the retraction movement from the drilled holes to allow the tool temperature measurement with the IR camera technique. The time delay between the generation of the cutting tool heat and the tool temperature measurements prevents the opportunity to perform an in-situ and instantaneous temperature measurement of the tool tip. The effect caused by this delay in the measurements was quantified and tackled by developing a numerical Finite Element Modelling (FEM) simulation. The developed FE model was used to estimate the temperature reached by the tool at the end of the drilling process (typically the highest temperature), starting from the tool tip temperature measured at the outlet. Since the PU material for biomedical experimentation is not aimed at mimicking also the thermal response of the biological bone (ASTM F1839 and - 08, 2012), the FE model was also used to investigate the differences in heat propagation between synthetic polyurethane bone and human bone.

2. Materials and methods

Cutting tests are performed in the laboratory on dental jaws made by commercial synthetic bone provided by Nacional Ossos (Brazil), consisting in rigid polyurethane (PU) foams, Fig. 4. These parts are indicated for surgical procedures such as cutting and placing plates, screws, or implants, but they are also widely used in basic implant placement courses and demonstrations. Despite their different thermal conductivity with respect to biological bones, synthetic bones are the best choice to obtain reliable and repetitive cutting results thanks to their controlled and constant material density. Moreover, these samples accurately mimic the physiological geometry of human jaws, allowing the proper design, adoption, and fixturing of dental guides. Polyurethane material can be found in different density levels (according to ASTM F 1839-08 (ASTM F1839, 2014),), and these grades should be selected to correctly mimic the target dental drilling operation of biological bone. Basing on previous studies from the authors, devoted to compare the performance and the cutting force generation of PU versus bovine and equine bones, it has been found that grade 15-20 could be an acceptable choice for the addressed dental drilling case under study.

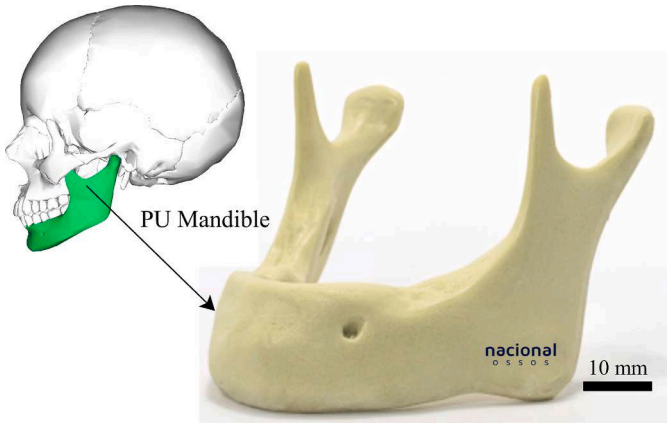

Fig. 4. Synthetic (PU) mandible samples adopted for the cutting tests.

Polyurethane jaws of the same type were then selected and utilized (12 units). Their geometry, weight and actual density of the different samples were preliminary measured by utilizing both destructive and non-destructive methods. It is confirmed that the density does not vary statistically within and between the samples, making them ideal for the experimentation.

2.1. Experimental set-up

An automatic drilling prototype system, Fig. 5, is designed, built, and adopted for laboratory scale testing to enable tight control of the rotational and feed velocities during the drilling operation to foster the heat generation's control and repeatability.

The tests were performed on a prototype Computer Numeric Control (CNC) cartesian machine with three moving axes and equipped with specific dentistry drilling equipment (Bien-Air, iChiro pro system (Bien-Air Dental IChiropro Surgery), with spindle connection diameter 2.35 mm, type 1, ISO 1797:2017). The system is equipped with custom-made fixtures that allow the holding of the dental spindle and the fixturing of the polymeric jaws. This latter is supported using a spherical joint system that allows three additional degrees of freedom that were used to setting up the correct inclination of the jaw for multiple holes. The spindle axis coincides with the tool rotational axis and was aligned with the guide holes prior to cutting. The system allows tight control of all the parameters of interest, such as feed rates, rotational speeds, and flow rate of irrigation water, including the opportunity to log the absorbed cutting torque. Dedicated G-codes are programmed to control the cutting tests.

Given the rigidity of the automatic machine adopted, position control assumes large importance. Any small deviation in the alignment positioning between the tool and the guide holes during the drilling operation can lead to increased friction of the two elements and consequent heat generation effects. This problem is of great importance because of the high rigidity of an automatic control machine. The surgical guides are in fact designed for manual surgery operations where the positioning is guaranteed by the surgeon's hand. On one side, the human control presented less positioning accuracy and reduced rigidity due to the muscular actuation, which helps the guide perform its alignment aid correctly. In fact, the guide is rigidly fixed to the maxilla/mandible bones, assuring more rigidity and stability with respect to human and drilling-induced force by guaranteeing a stable positioning during all the drilling operations. Therefore, to minimize these unwanted effects, given by the high rigidity of the spindle motion, it was decided to provide a designed elastic compliance to spindle fixturing, trying to mimic the inaccurate surgeon's motion. This was implemented by interposing an elastomeric band with 3 mm thickness between the dental spindle and the spindle holder.

Regarding the direct temperature measurement with contact method, a K-type thermocouple (with an accuracy of ±1.1 °C, diameter of 1.6 mm) is placed inside the jaws, Fig. 6, and acquired through a data acquisition system and MATLAB software. The sensor is inserted inside the samples through a guiding hole with a 7 mm depth. These holes for the thermocouples were drilled right before the dental drilling test execution by using the same dental spindle equipped with a dedicated pilot drill bit). The border-to-center radial distance between the main hole in the jaw and the sensor position was kept at 1 mm. A high-

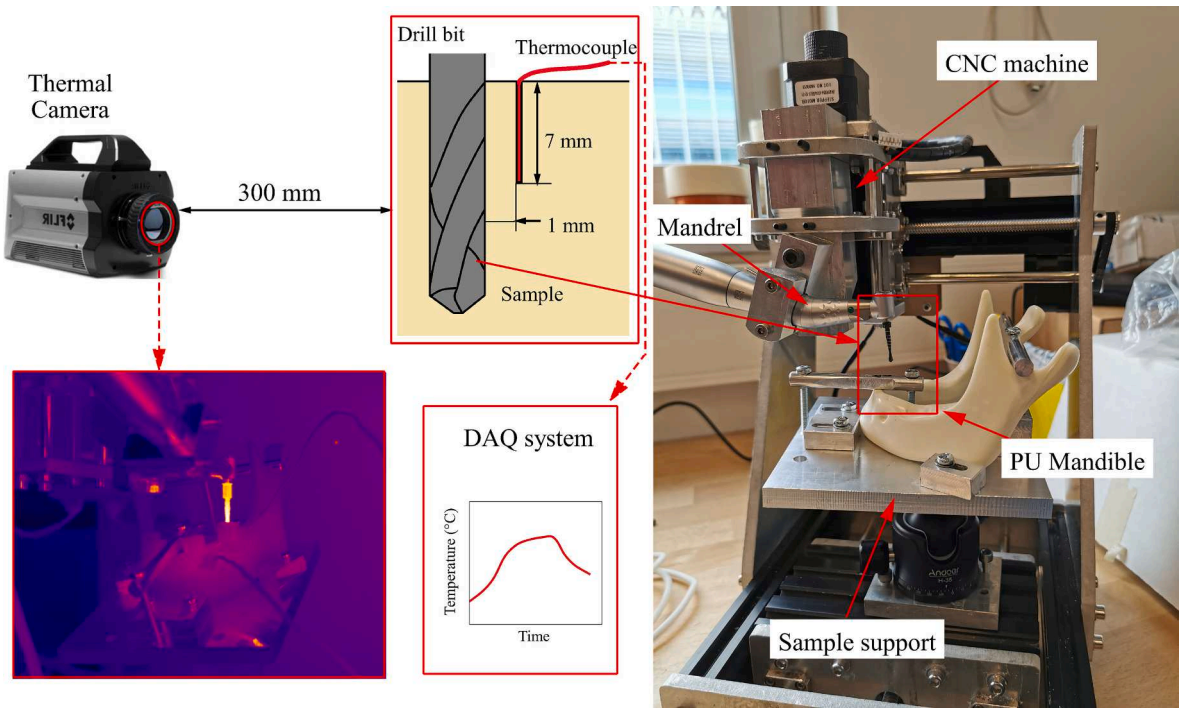

Fig. 5. Experimental setup used for the dental drilling tests.

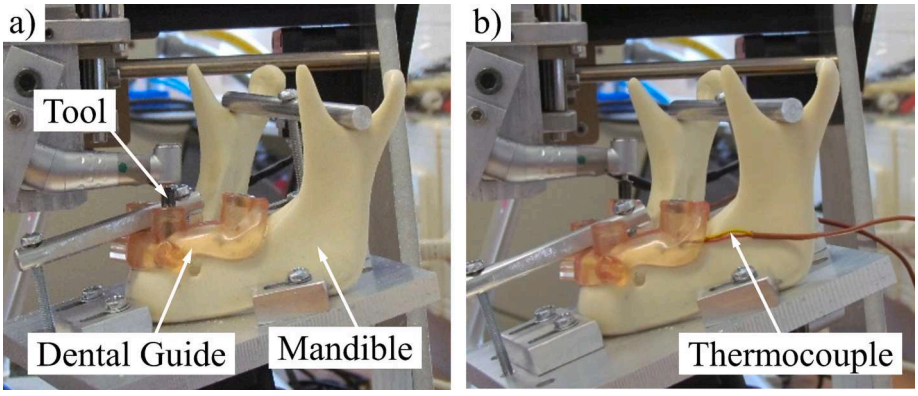

Fig. 6. Experimental set up (a) without thermocouple (for alignment), (b) with thermocouple (for temperature measurement).

performance thermal paste, MX-4 (Arctic GmbH, Germany) was used for the thermocouple coupling. An infrared camera FLIR SC6100 (FLIR systems, Sweden) equipped with a 25 mm lens was used for the indirect temperature acquisition method used to quantify the temperature reached by the drill bits. The camera was placed in front of the cutting system (orthogonally to the X-Z plane of the moving axes) aligned with the vertical position of the jaw, at a focus distance of 300 mm, and framing both the spindle, the drilling bit, and the jaw for all the duration of cutting tests. The sensor was calibrated by finding the emissivity coefficient of the framed materials. The parameters of the infrared camera are the following: i) Temperature range: 10 °C – 90 °C; ii) Resolution: 640 x 512 pixels; iii) Integration time: from 10 μsec to 687 s; Frame rate for video acquisition: 120 Hz; Measurement and analysis accuracy: ±1 °C.

2.2. Testing procedure

Usually, dental drilling surgeries employ a sequence of different drilling tools with increasing diameters and lengths to control the accuracy and heat generation depending on the type of bone density of the patient. Therefore, the procedures for the realization of the holes are different in the case of bone D1, compared to D2, D3, and D4, according to Misch's classification (Misch, 2007). In all the cases, the first drilling phase consists of the realization of the pilot hole using a drill bit called a lance drill to carve the cortical bone. Following the pilot hole, the dentist continues the drilling process using different tools, each one having a slightly larger diameter and length, until the correct values for the implant are reached. Usually, surgical tool manufacturers prescribe an abundant use of external irrigation with saline solution, or sterile distilled water, and peck (intermittent) drilling strategies during the whole operating phase. There are cases however where dry cutting can be prescribed simplifying the surgery operations. In commerce, the implants are typically sold with a surgical kit containing all the components, particularly the different drill bits necessary for the surgical operation. Indeed, there is a difference between bits used for classic drilling and guided drilling procedures. The latter types feature a guiding shoulder present on the tool shank. This feature allows the correct coupling of the tool with the dental guide and tight control of the drilling depth (thanks to an upper lip that acts as an axial limit to the tool's vertical travel). The shank has the same nominal diameter as the

bush in the guide, allowing the perfect alignment and inclination of the implant hole.

The experimental testing developed in this work pivots to using two different commercial surgical kits for guided dental surgery following two different guiding approaches, Type A and Type B. The first system, Type A, is characterized by a resin jig that embeds metallic bushes into the guiding zones. The supplier suggests dry cutting, thanks to the adoption of Diamond-like carbon (DLC) coating present on the tools and prescribes a generally low cutting speed. In this solution, the coupling between the metallic bushes and the tool shanks happens with a constant diameter, independently from the final size of the adopted tool. In the second system, Type B, a fully polymeric jig is adopted. In this solution, uncoated stainless-steel tools are adopted therefore suggesting water supply as coolant. The bushing system adopted is different from Type A since external metallic adapters are used in Type B that allow the correct fitting of the different-sized tools in the resin holes.

2.2.1. Type a guide solution: dry cutting with internal bushings

The Type A jig is constituted by a premium-quality surgical guide dental resin, a material designed to print at 100 μm and 50 μm layer line resolutions on commercial stereolithography printers (SLA), Fig. 7 a. Its material characteristics are illustrated in Table 4 (Appendix). The guide presents 4 holes and internal metal bushings obtained by inserting in the resin component nut bushes in stainless steel material with a diameter of 5 mm and length of 7 mm. The clearance between the tool shank and the guiding bushes is measured in approximately 0.1 mm. The tools are made in stainless steel DLC coated to reduce friction with guide bushings as well as with the cutting bone material. Thanks to this feature, these tools are prescribed for dry cutting operations. They are characterized by a connecting shank of 10 mm length, according to ISO 6360-1, which allows the tool to be accommodated in the tool holder. A flange is present on the tool to lock the tool insertion length inside the guides, thus allowing fine control of the drilling depth during the surgery. Preliminary testing confirms that due to the tool holder clearance, the tools are not rigidly held by the spindle and this radial play generates a radial runout at the tool tip quantified in maximum 1.2 mm for the longest drills. The jig geometry was designed to adapt to the polymeric jaws described above. An all-on-four technique was mimicked by adopting two sets of holes for a total of four holes distributed evenly along the jaw. Three (3) jaws are cut for a total of 12 holes for each of the two guiding surgery methods tested (namely, the free and the guided condition) with 6 jaws in total and 24 holes. The Type A kit consists of tool 1 (twist drill bit $\Phi = 2.3$ mm; $L_{max} = 8.5$ mm, point angle = 92.5°, 2 cutters), tool 2: (twist drill bit $\Phi_1 = 2.9$ mm, Φ_2 3.8 mm, $L_{max} = 8.5$ mm, 3 cutters) and tool 3 (twist drill bit $\Phi_1 = 2.9$ mm, Φ_2 3.8 mm, $L_{max} = 15$ mm, 3 cutters), Fig. 7 b. Where Φ is the diameter of the tool and L_{max} represents the max tool penetration depth inside the guide. A partial randomization of these tests was performed between the six jaws to minimize any unknown and left side effects caused by mandible material and geometrical variability.

2.2.2. Type B guide solution: wet cutting and external adapters

The Type B guides are realized by means of the *Objet30 OrthoDesk 3D Printer*, a professional desktop 3D printer designed for small orthodontic labs and clinics, Fig. 8 a. Biocompatible *VeroGlaze™ (MED620™)* material was adopted as an opaque white resin material, medically approved for temporary in-mouth placement up to 24 h. Its material characteristics are illustrated in Table 4 (Appendix). The specific surgical kit of Type B solution consists of the different drilling bits with increasing diameters. In this solution the tools are coupled with dedicated metallic reducers (basing on the tool diameter, see Fig. 8b), which allows to fit the different tools in the same surgical guide, which is made only by resin material without the presence on any internal metallic bushings. In this solution, the drilling bits are made of uncoated surgical grade stainless steel (DIN 1.4197- 420F Mod), a highly biocompatible metal that reduces the risks of allergic or inflammatory reactions. With respect to Type A tools, whose shapes are characterized by zones at different diameters, the Type B tools have more constant diameters and less mass than the previous ones.

A reduced subset of three bits was selected from the available tools contained in the commercial kit, as a representative subset. In particular, the tool 1 consisted in a launch drill bit Φ 2 mm, $L_{max} = 4$ mm (center drill), the tool 2 in a twist drill bit Φ 2 mm, $L_{max} = 13$ mm and the tool 3 in a twist drill bit Φ 3.25 mm, $L_{max} = 13$ mm, Fig. 8 c. The representative cycle depicted in Fig. 3 refers to the selected Type B tool sequence. Fig. 9 represents schematics of these two guiding solutions type A and B.

In the Type B kit distilled water was used, by injecting it through the mask channels by a syringe manually operated. Water was brought at a temperature 3 °C lower than room temperature. In real surgery practice, water can be supplied at much lower temperature (up to 18/20 °C less than ambient temperature) so that a worse condition is studied. Five different jaws were adopted giving rise to a total number of 20 drilling tests. Among these, 10 holes were performed in guided conditions and 10 in standard free cutting configuration. The same randomization performed with Type A set was adopted. Table 1 shows the process parameters and experimental conditions. Fig. 10 shows the Material Removal Rates (MRR) versus the cutting duration of each drilling step for the two types of configurations. In this figure, the area of the rectangles represents the resulting potential heat generation for each tool and condition, since the higher MRR, the higher is the expected heat flux and the higher the cutting duration, the higher the contact time and then the temperature increase. Basing on the nominally adopted cutting parameters, the tests revealed that tool 3 is prone to generate the highest

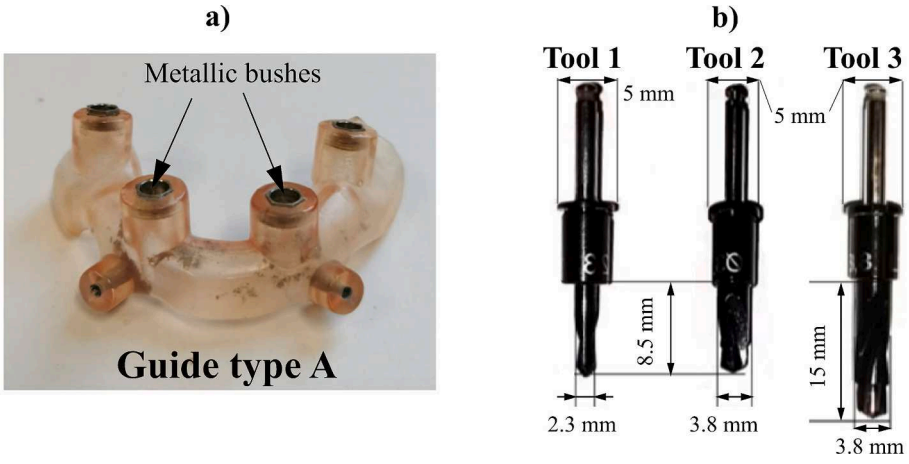

Fig. 7. (a) Surgical guide template for Type A, (b) Surgical drilling tools for Type A (MULTYSYSTEM S.p.A., Lissone, MB, Italy).

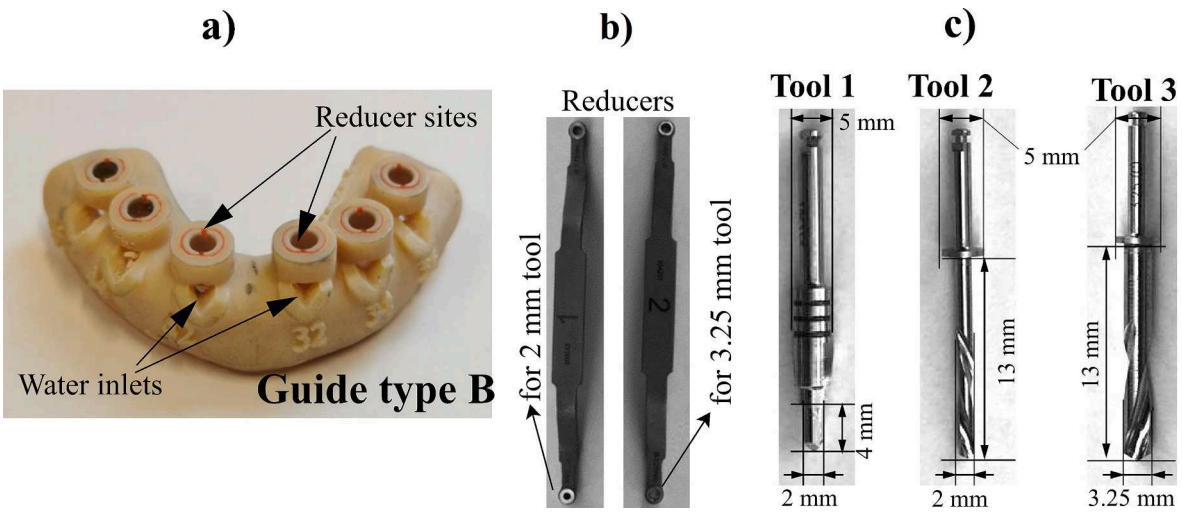

Fig. 8. (a) Surgical drilling tools for Type B (Zimmer-Biomet, Zimmer INC, Warsaw, USA), (b) Surgical guide template for Type B and (c) metal reducers for Type B.

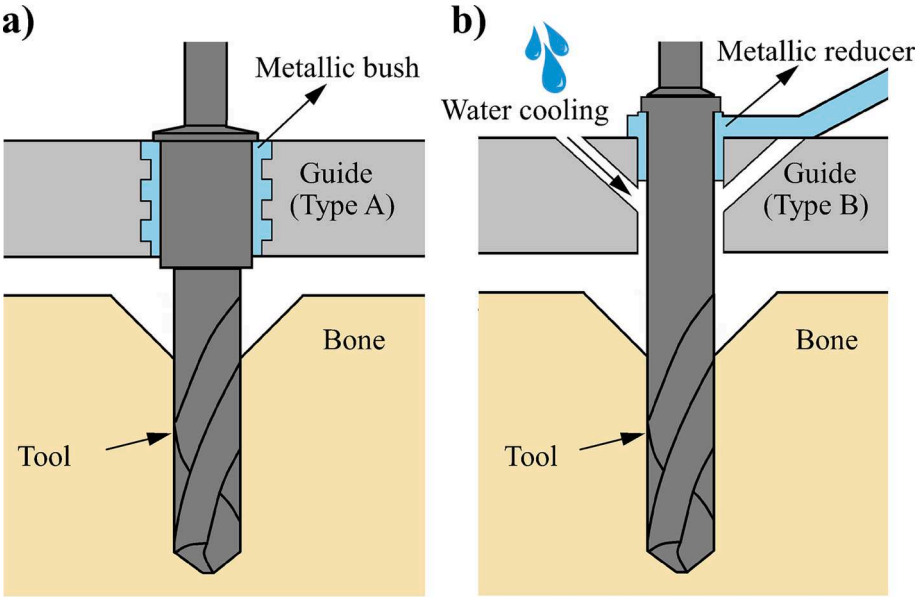

Fig. 9. The representation of the (a) Type A and, (b) Type B surgical guiding principles.

Table 1
Cutting parameters of the tested experimental procedures for the two guide solutions (Type A and Type B).

Guiding type	Diameter [mm]			Max cutting length [mm]			Rotational speed [rpm]			Feed rate [mm/s]			Material removal rate (MRR) [mm^3/min]			Total material removed [mm^3]		
	Tool number																	
	1	2	3	1	2	3	1	2	3	1	2	3	1	2	3	1	2	3
Type A	2.3	3.8	3.8	4	8.5	15	400	1	249.3	563.2	680.5	16.6	79.8	73.7				
Type B	2	2	3.25	4	12	12	700	1	188.5	188.5	309.26	12.6	25.1	99.5				

temperature with respect to tools 1 and 2. Due to these factors, the focal point of the results section in this study primarily revolves around tool 3. This tool not only exhibits a high material removal rate, but it also serves as the final step in the multi-step drilling approach. Consequently, it is expected to have the greatest impact on bone thermal generation since in the final phase, the bone material accumulates the heat generated during the preceding drilling steps.

3. Results

3.1. Air-tests (only tool rotation without any drilling)

The "air cutting" experiments are designed to decouple the two main sources of heat generation, namely the friction of the tool with the bushing and the drilling generated heat. The heat generated by the contact between tool and the bushing is then quantified for the two types of guides. Fig. 11 shows the thermal generation due to bushing friction

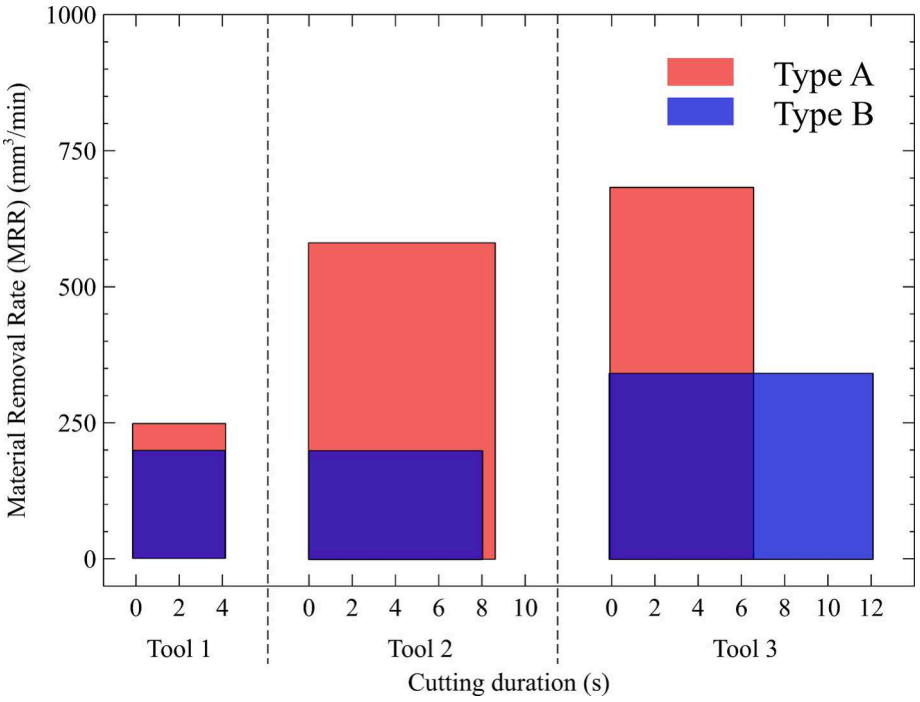

Fig. 10. The representation of Type A and Type B drilling solutions.

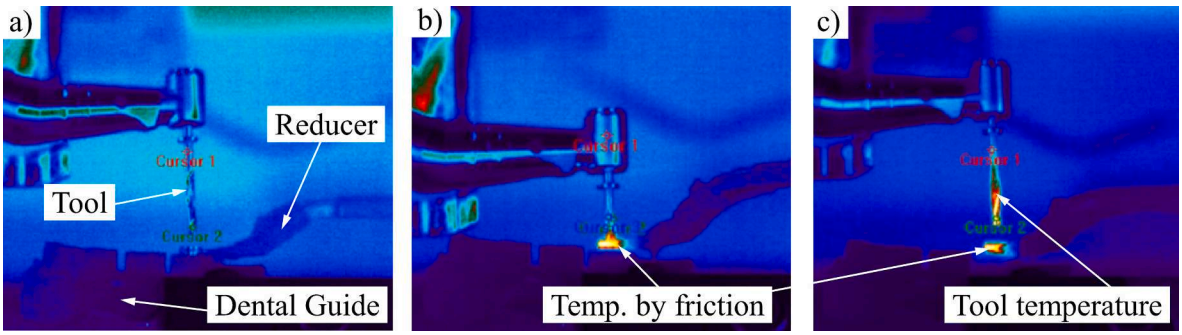

Fig. 11. Thermal camera pictures during air tests with the Type B guided solution: (a) the tool is disengaged but rotating, (b) the tool engages with the guide, (c) the tool disengages after the drilling.

for a representative Type B case.

The rotational movement of the tools in the air produced an average reduction of about 0.5 °C of the temperature, both for Type A and Type B tests, Fig. 12. This negligible effect is caused by the fact that the tools once installed in the spindle have a little higher temperature than the surrounding environmental air that therefore introduces this little cooling effect by convection.

Instead, when the tools are inserted into the bushings and are put in rotation (but not cutting the bone), there is an higher average increase of the tool temperature. This effect is introduced by the solely friction with the surgical guides bushes/adapters and resulted equal to 1.8 °C for Type A and 1.4 °C for Type B. In this data, a greater temperature dispersion was shown in the Type A tests (std.dev. = 3.3 °C), where the embedded metal bushings were adopted, Fig. 12. This could be linked to the alignment effects created in the tool-guide couplings. Despite the presence of the clearance between the tool shanks and the bushings for both Type A and Type B, the former type's bushes are internal and therefore they have limited capacity to self-align when in contact with the tool. Moreover, the type A bushings present bigger diameters and longer couplings in axial direction with respect to Type B ones, which determines a stiffer coupling and larger friction area. Instead, in the type B solution, the manual holding of the adapters allowed additional degree of movements of the bushing during drilling which could have helped in damping the effects of the alignment and better compensate for the system rigidity. In any case, the maximum increase of tool temperature during simple rotation in the bushing (but without drilling the bone) registered was 5.3 °C for Type A conditions.

3.2. *Drilling tests*

The results of the drilling tests on the synthetic PU bone are analyzed in terms on temperature increase both on the PU material as well as on the tools. For this latter, the difference between the maximum tool temperature reached during the drilling testing and the baseline tool temperature measured right before starting the cutting procedure, is considered.

3.2.1. *Effect of the surgical guides on the PU bone material temperature: thermocouple readings*

Fig. 13 depicts a representative temperature–time series data measured by the thermocouple installed on the PU jaws. It is confirmed that the last drilling step conducted by tool 3 is the one generating more heat into the specimens, unconditionally for Type A and B.

The registered temperature increase is limited, about maximum 4 °C

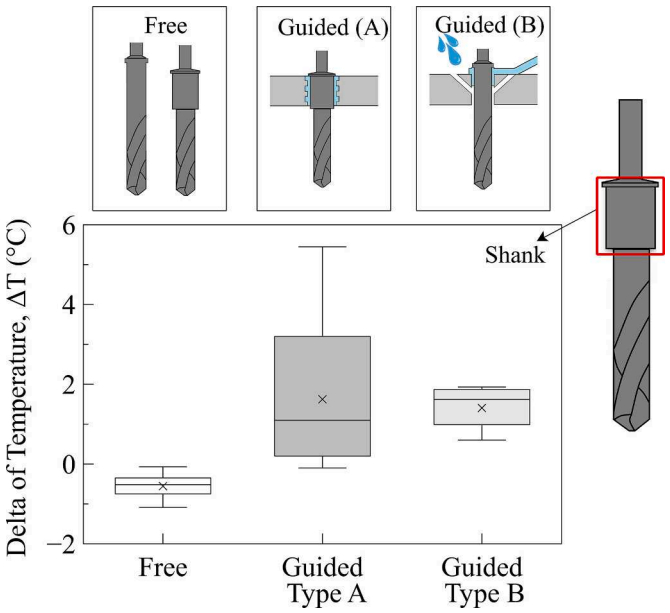

Fig. 12. The experimental temperature data measured from tool's shank during air tests (no drilling).

in all the conditions tested, for both type A and Type B. In that range, the maximum temperatures read by the thermocouple during the tests are also affected by a large variability which prevents a sensitive evaluation of the difference between Type A and Type B and of the effect of the guide presence.

The limited temperature elevations of the PU material measured by the thermocouple (TC), can be attributed to the material's low heat conduction capacity. Due to the insulating characteristics exhibited by the Polyurethane, the dissipation of drilling heat is significantly hindered becoming spatially limited (all the heat remains located near the drilling site), making the TC sensors not capable to capture the heat flow. This is true also when TCs are positioned closer to the hole surface. The temperature recorded by the TC exhibits minimal increments during the drilling process, while also displaying significant variations between many tests. This phenomenon can be attributed to the localized distribution of heat within the samples. Due to this high thermal gradient, caused by the low thermal conductivity of PU, the sensitivity of thermocouple readings is greatly influenced by the placement of the sensor, with even little variations resulting in significant differences in the recorded thermocouple readings.

Furthermore, tests conducted without the guiding often exhibited reduced positional accuracy of the holes, in relation to the intended controlled position set by the CNC machine, introducing variability in the TC readings between repeated tests. Since the positional capacity of the adopted CNC machine was high, much higher than the human ones, the shown inaccuracies were primarily attributed to the clearance exhibited by the tools in the tool holder of the spindle.

3.2.2. *Effect of the surgical guides on the spindle drilling torque*

The spindle torque data for guided and free (non-guided) conditions are depicted for type A procedure in Fig. 14. From these signals, it is shown that both the temperature and the torque values for the tool 3 are greater than the tool 1 and tool 2 for guided and non-guided conditions and this confirms the expected greater impact of tool 3 from the thermal viewpoint.

Overall, in terms of the effect between the free and guided conditions, no sensible variations are observed in the torque signals. Little variations are observed in the profiles of the torque of the tools 3 but the maximum reached torques are not varying sensibly (those variations were lying within the limited resolution in the spindle torque reading, i.e., 1 N cm). These data confirm that the clearance adopted between guide bushing and tool shanks are therefore enough to guarantee a regular and free rotation of the tool and that the friction generated in the contact, cannot be captured by the spindle torque, namely.

3.2.3. *Effect of the surgical guides on the tool temperatures: thermal camera measurements*

Considering the aforementioned limitations of the TC readings on the jaws, the effect of the presence of drilling guide is evaluated in terms of indirect temperature measurement on the tools by adopting thermal camera readings. Fig. 15 displays the thermal pictures of the cutting as measured by the thermal camera under both guided and non-guided

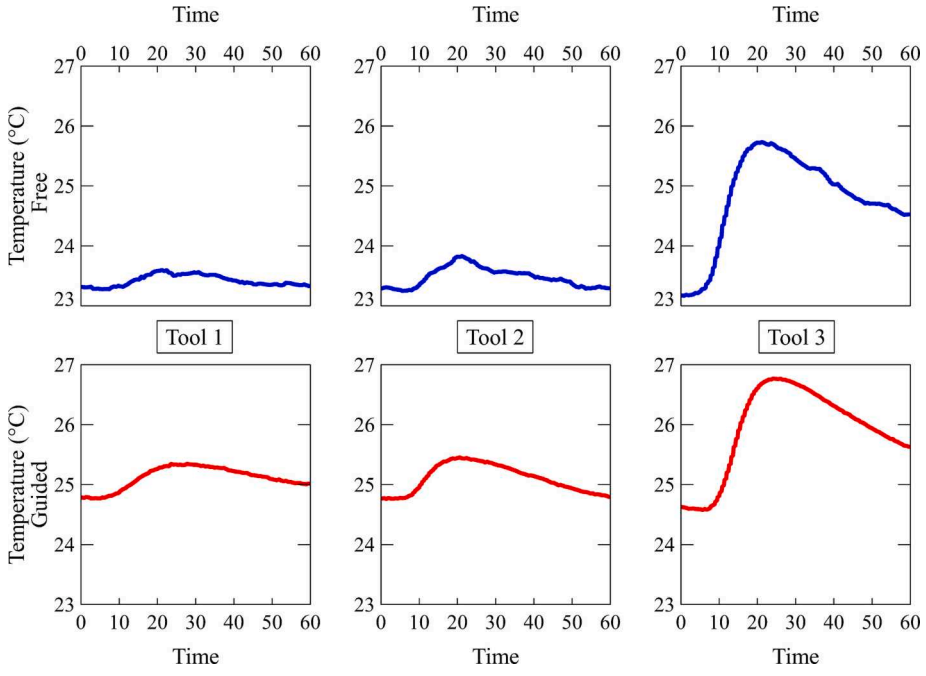

Fig. 13. Thermocouples reading during the Type A multi-step drilling solution. Free conditions (above), guided conditions (below).

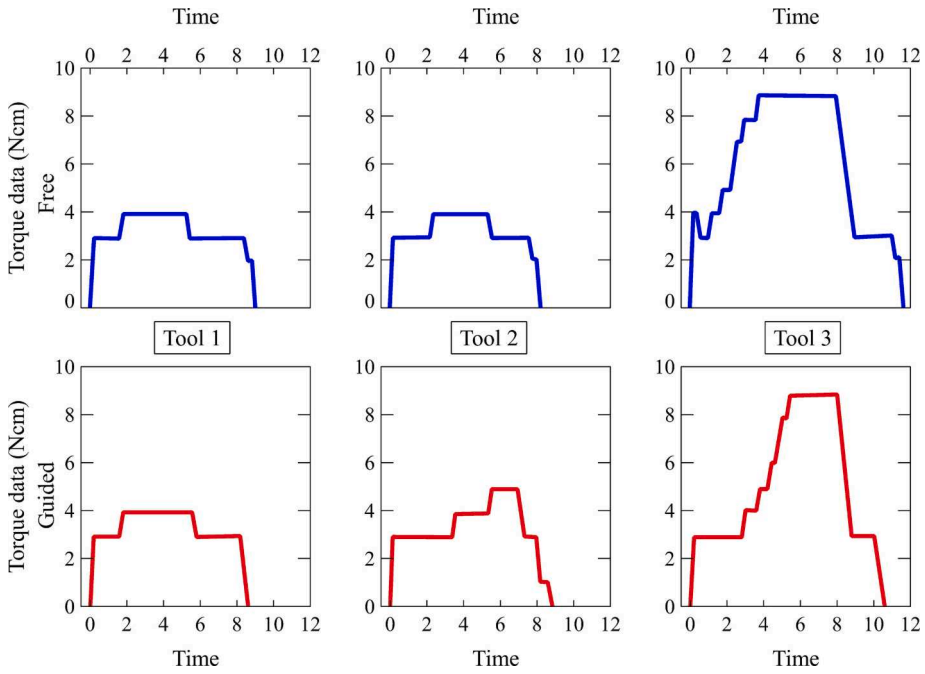

Fig. 14. Spindle torque during free and guided cutting in Type A solution.

settings (Type A). More in details, Fig. 16 shows the extracted tool temperature profiles in the free and guided conditions, right after one representative conducted drilling test. From these data the synthetic information about the tool temperatures increases (in terms of delta of temperatures) are extracted and compared for the free and guided case, Fig. 17.

By analyzing the temperature of the tool, measured right after the tool extraction at the end of the cutting tests of Type A (in dry cutting condition), it is confirmed that cutting tools reach a much higher temperature with respect to the measured PU material temperature, in the range of 45-55 °C. As expected, the heat accumulates more on the cutting edges and propagates through the shank, Fig. 16. Part of this heat is accumulated also on the PU material, Fig. 16a and on the guiding system, Fig. 16b. In the case of guided condition, the heat distribution along the axial direction on the tool is more homogeneous and involves the tool shank in contact with the guide bushing. In this zone, the temperature is typically lower than in the tool tip zone, even if the little control flange posed at the top of the tool shank (whose aim is to limit the axial immersion of the tool in the guide) is subject to higher temperature increase.

In terms of differential values with respect to base tool temperature, the data provides a clear picture of the situation, Fig. 17.

An average increase of 2.7 °C is generated on the tool shank Type A during the non-guided cutting procedure. Conversely, the average increase reached up to 4.6 °C with guided drilling (Fig. 17a). The average temperature increase in the cutting helical zones reaches 17.9 °C and 18.5 °C in the non-guided and guided drilling, respectively (Fig. 17b). The maximum increase in that zone is noticed for guided drilling at 25.7 °C, while the minimum average increase is 12.5 °C for the same condition. Still, a higher data dispersion can be noticed when using the guides due to the variability in the positioning of the tool axis with respect to the metallic bushing (guided). This aspect was discussed already in the air testing.

Interestingly, by looking at the air testing and the drilling tests, Figs. 12 and 17 respectively, it is possible to note that the sum of the two heating components, the one caused by the tool-guide bushing friction (see "Guided Type A″ in Fig. 12) and that caused by the cutting process in the free condition ("Free" in Fig. 17), is similar to the average delta of temperature recorded in the guided drilling procedure (see "Guided" in Fig. 17). This suggests that the heat generation in the system can be considered decoupled, meaning that the above-mentioned heat sources seem to contribute independently to tool temperature increase.

On the opposite the Type B case shows a different situation. In this scenario, the three different tools are with an external coolant system based on water at $T = T_{room} - 3$ °C.

The reached tool temperatures are generally lower than Type A

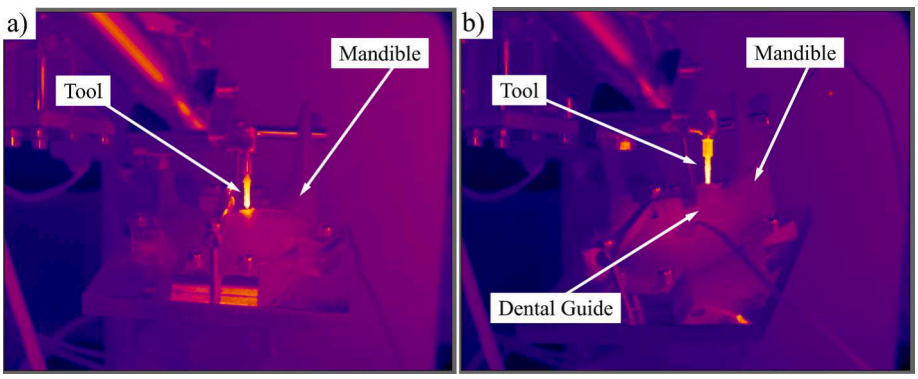

Fig. 15. Thermal camera images during free (a) and guided (b) drilling with Type A solution.

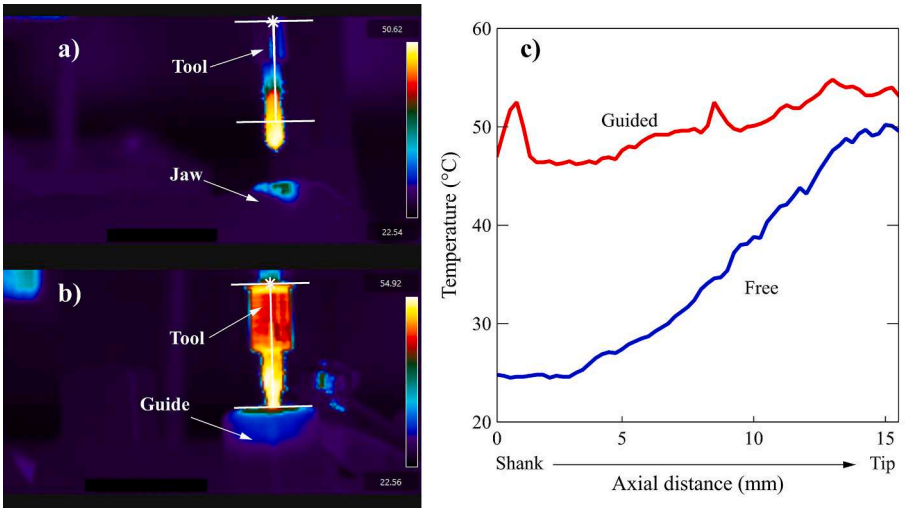

Fig. 16. Temperature generation measured without (a) and with (b) the guide Type A tool 3, by thermal camera.

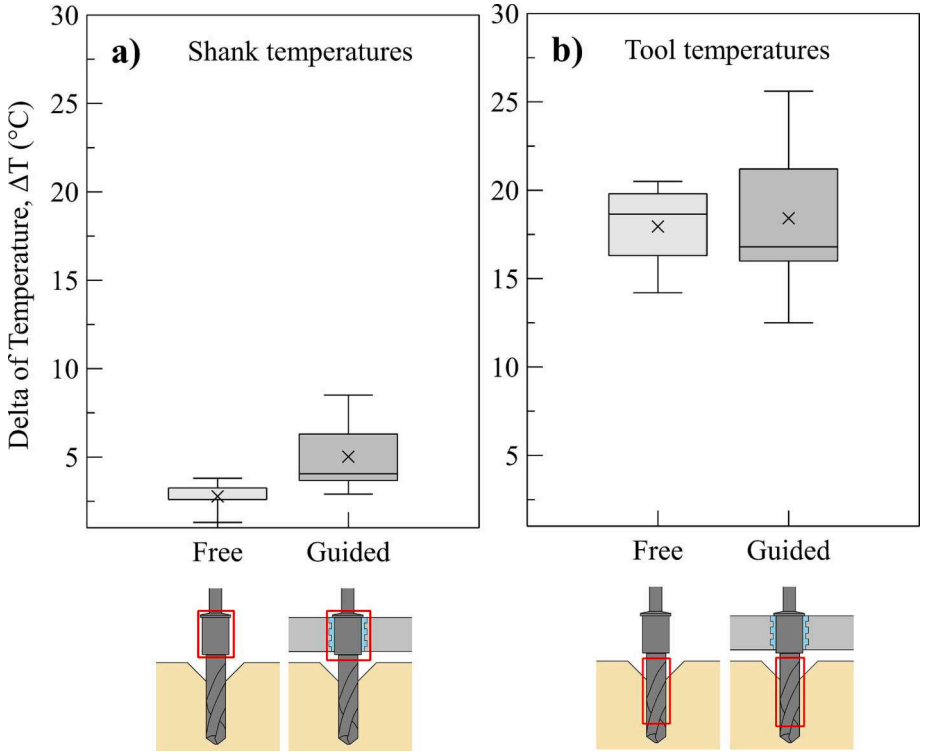

Fig. 17. Increase of tool temperature measured with thermal camera in Type A solution (Free: cutting using tools Type A but without guide, guided: cutting using tools and guide Type A). (a) temperatures of tool's shank, (b) temperature of tool (average between body and cutting edges).

condition, namely in the range of 20-35 °C, Fig. 18. The variability between the reached tool temperatures in the Type B results more limited than Type A condition, allowing to identify a clear distinction between the guide and free drilling condition for all the three tested tools. Interestingly, the contribution of the guiding system appears to be similar for the three tested tools, despite the different diameters of the tools and the external adapter bushing systems.

By analyzing the values collected on the tool shanks, it appears that the increasing temperature effect of metal reducers cannot be compensated using the coolant due to the guide's geometry that prevents fluid from reaching the shank (Fig. 19a). On the contrary, the usefulness of the coolant can be seen in Fig. 19 b: the direct water jet on the tip of the tool allows an important temperature reduction, which results in a temperature lower than room one in conditions of traditional implantology and in a temperature only 1 °C warmer than room temperature in guided technique.

In particular, the values recorded on the shank are shown in Fig. 19 a, while the values referred to the tool body are reported in Fig. 19 b. By analyzing the temperature values, the tool shank Type B generated an average increase of 0.5 °C during the non-guided cutting procedure. The average increase reached up to 2.8 °C with guided drilling. Conversely, the average temperature increase in the cutting helical zones reaches -2.1 °C and +1.2 °C in the non-guided and guided drilling, respectively.

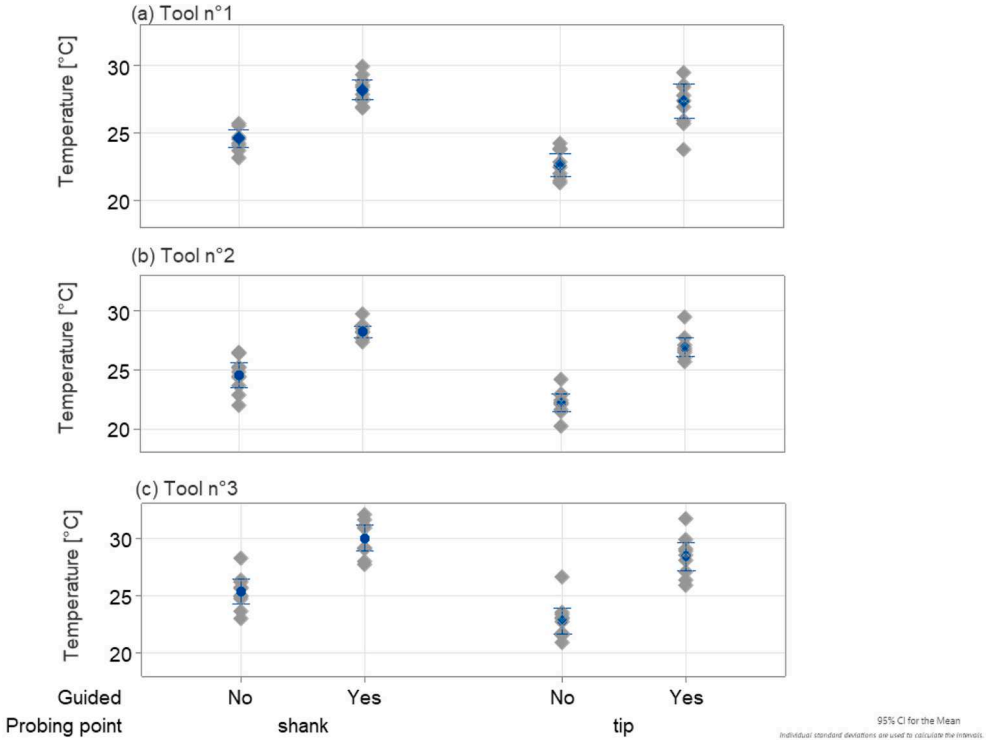

Fig. 18. Thermal camera temperature readings during Type B experiments (free and guided drilling).

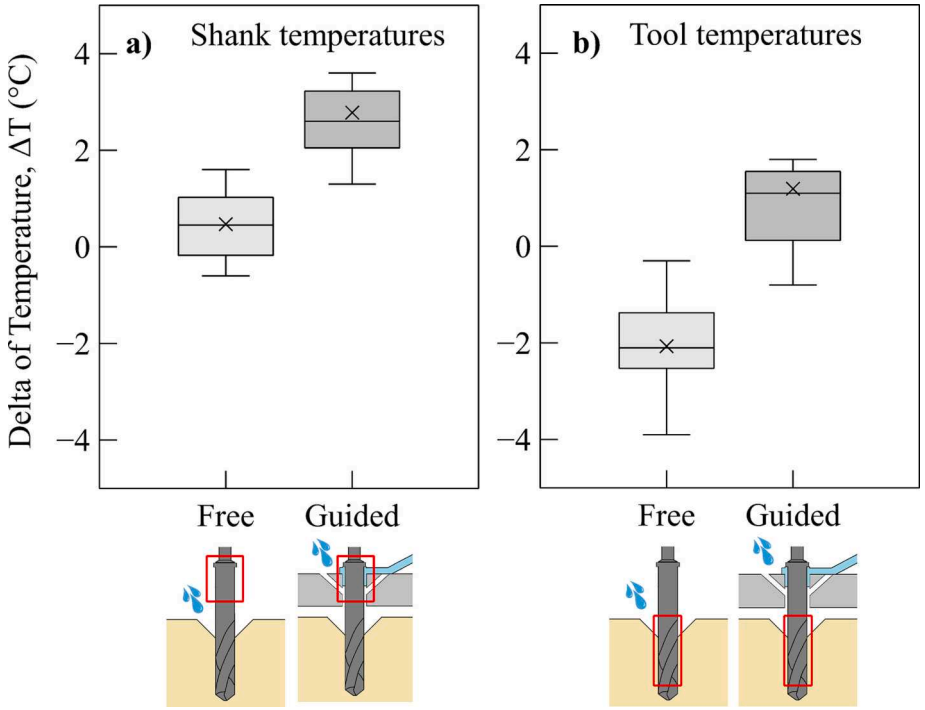

Fig. 19. Increase of tool temperature (delta) measured with thermal camera in Type B solution (Free: cutting using tools Type B but without guide, guided: cutting using tools and guide Type B). (a) temperatures of tool's shank, (b) temperature of tool (average between body and cutting edges).

4. Numerical investigations for temperature increase on PU and human bone

The conducted experiments on PU material allowed the quantification of the thermal effect introduced by the guiding system on the drilling tool temperature. Given the limitations of the adopted thermal sensing approach, based on the infrared imaging applied on the tool, this evaluation however refers to the temperature of the tool right after the cutting, namely at the tool disengagement from the hole. Indeed, the maximum tool temperature reached during the drilling operations could not be outlined via the experiments. On the other side, regarding the temperature reached on the workpiece material, being the PU, a low

conductive material characterized by different thermal properties than the patient bone, the collected thermocouples measurements on the synthetic jaws cannot reveal what would happen if the operation were done on living human bone. Medical grade polyurethane is in fact very accurate to simulate human bone in mechanical tests; however important differences exist considering thermal behavior as highlighted in Table 2.

To estimate whether the increase of material temperature introduced by the guiding system contributes to an increased risk of tissue damage and bone necrosis in patient biological bone, a numerical approach is used in this work, whose main steps are illustrated in Fig. 20.

In particular, a FEM (Finite Element Modeling) numerical simulation is used to identify the maximum tool temperature reached on the tool when it is drilling inside the samples, starting from the experimental thermal camera readings (which have been acquired after the drilling during the tool retraction). Then, starting from information, an estimation of the thermal disturbance in living bone is performed identifying the time domain profiles of the temperature evolution and the potential thermal damage to the surrounding tissues.

Two main objectives are therefore addressed with the proposed FE models:

1. Obtain the actual maximum temperature generated on the drilling tool tip (overcoming the limitation that affects the experimental measures).
2. Investigate the differences in heat propagation between synthetic (polyurethane) bone and human living bone material.

The fundamental concept behind both objectives is to adjust the heat input of the FE model using the experimental tool temperature values. In other words, it carries out an indirect estimation of the heat flux that flows through the tool to support the thermal camera's temperature data. A temperature input is set on the FE model for the contact region between the tool and the guide beginning from the estimated heat flux. This results in an estimation of the temperature in the time domain for both the material of the tool and the workpiece. It should be emphasized that the existence of the drilling guide is indirectly modelled in the FE model (rather than as a physical component) by setting the aforementioned heat flow level.

4.1. Implementation of the FE model

A representative drill bit geometry is modelled, Fig. 21, by adopting the main geometrical characteristics of the drilling tools used in the experiments. In particular, the size of the largest drill bit (Fig. 8a) used in Type A experiments (cutting length = 15 mm, chisel angle = 115°, maximum diameter = 3.8 mm, material = AISI304 with DCL coating) is modelled. As discussed above, the reason for this selection is because this is the tool with the higher MRR and so the one that is expected to generate more heat.

The tool is divided into two areas: zone 1 (tool tip), and zone 2 (shank). In the former zone, the cutting heat is simulated by imposing a known temperature of the cutting edges. In the latter, the friction heat generated by the sliding between tool shank-bushing system is taken into consideration (Fig. 21). The simulations are performed through the software ANSYS by adopting a "Transient Thermal" analysis. According to the transient thermal model, the heat conduction through a solid is given by following governing equation:

$$k\left(\frac{\partial^2 T}{\partial x^2}+\frac{\partial^2 T}{\partial y^2}+\frac{\partial^2 T}{\partial z^2}\right)+q=\rho c\frac{\partial T}{\partial t} \quad \text{Eq.(1)}$$

In the Equation (1), k is the thermal conductivity ($W/K\bullet m$), t is time (s), T is the temperature (K), q is the rate of heat flux/convection/radiation/internal heat generation inside the volume (W), ρ is the density of the material (Kg/m^3), c is the specific heat of the material ($J/Kg\bullet K$). It is understood from the equation that transient thermal analysis helps to determine temperatures and other thermal quantities that vary over time.

The simulations durations are set to mimic the entire drilling operation namely, 14 s, from the beginning of the drilling tool motion to the moment of the temperature measurement (taken with thermos camera in the experiments).

A delay of 7 s is considered to define the thermal cycle of the FE model, as the time between the tool in the bottom hole position, and the tool tip measurement by the thermal camera when the tool retracted from the hole. The assumption here is that the tool does not produce heat while disengaging the hole axially (no thermal contributions from the drilling bit margins, namely no thermal generation contributes along the axial contact with the hole surfaces).

Initial temperatures are very important in transient analyses because they affect the whole analysis. In this case, the workpiece material is set at 22 °C and 37 °C to mimic the laboratory testing on the PU material and the in-vivo testing of living bone, respectively.

As boundary conditions, a constant temperature is set on the cutting edges in the tool tip (zone 1), that represents the heat generation during drilling. The temperature, namely the heat source, is activated for the entire duration of drilling process (7 s) and then deactivated. This procedure is simplified with respect to the complete thermal generation modelling of the bone drilling which would requires an extensive range of parameters and variables to be implemented (Sui et al., 2015). A convection term is activated on the entire tool body for the last 3 s of the simulation, to mimic the cooling of the tool during retraction (air convection coefficient = 5 $W/K\bullet m^2$). As already introduced, the temperature value in zone 1 is found through a trial-and-error approach by comparing the numerical and experimental results (see results section). The simulated temperature value varies until both the shank and the tip temperature values obtained from experimental thermal camera readings are matched in the simulation (for both the cases, with and without the surgical guide).

To summarize, the defined cycle consists in:

- 7 s of active drilling time.
- 3 s to retract from the sample.
- 3.75 s (rounded to 4 s) to move the tool at the axial coordinate where its temperature is measured by the probe (to mimic the thermal camera readings).

The maximum temperature reached by tool tip are then identified with this FE model and this information are exploited in a sequent numerical investigation to predict the spatial heat distribution on the mandible models and the differences between polyurethane and human bone behaviors.

In these second numerical investigations, multiple FEM analyses are carried out on a simplified model of the mandibles to optimize computational effort. The movement of the heat source, namely the drill bit tip, is represented by grading the activation of the temperature in the hole. This is done by dividing into 12 sections (with 1 mm height) the drilled holes and the temperature is progressively activated on the surfaces of each considered sectional ring for 1 s, until the tool reaches the bottom hole position, Fig. 22. The sequential activation is done starting from

Table 2
Materials properties[a] considered in the FE model.

	Polyurethane	Human bone
Density [kg/m^3]	564	320
Thermal conductivity [$W/m\bullet K$]	0.03	0.3
Specific heat [$J/(kg\bullet K)$]	1350	2274
Thermal diffusivity [m^2/s]	$3.94\bullet10^{-8}$	$4.12\bullet10^{-7}$

[a] All constants are assumed temperature-invariant in the tested temperature range.

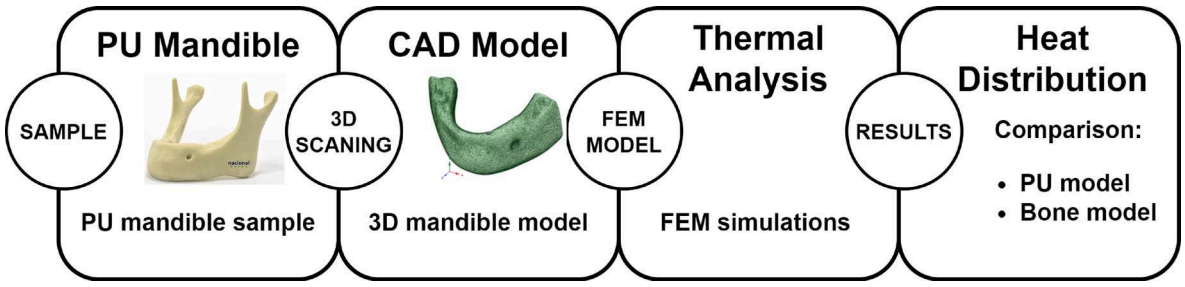

Fig. 20. Flow-chart of the FE modelling.

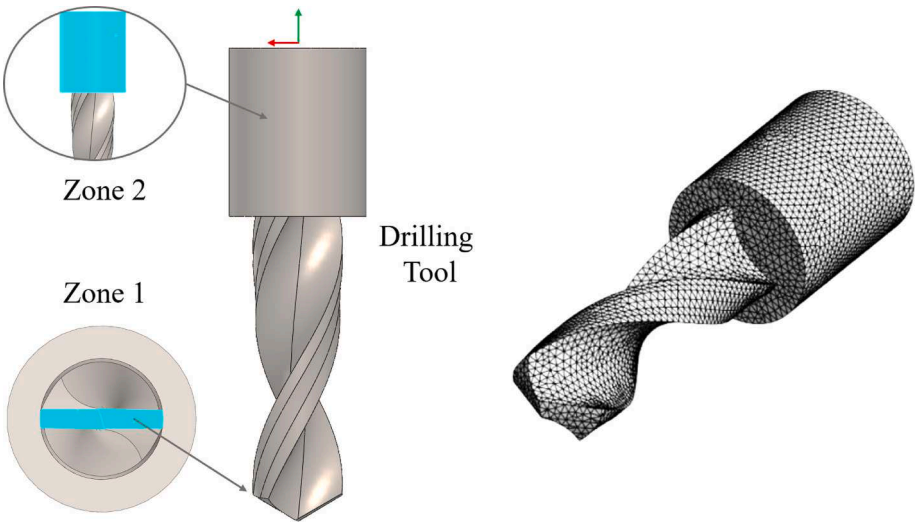

Fig. 21. Drill bit FE model and temperature measurement zones considered.
The workpiece material model consists in a homogeneous material whose properties depend on the material considered (PU or biological Bone) taken from literature (Davidson and James, 2000; Tissue Properties).

partitions 7 to 12 according to the engaged condition of tool (see Type A in Table 1). The temperature value at which the surface ring of the hole is activated is assumed to be the temperature on the tool, obtained from the previous simulations. The assumptions here are that the tool perfectly transfers its tip temperature in radial direction to the material (no axial thermal generation) and that the bit temperature remains constant during the tool penetration. In these second set of simulations, air convection is set also to the external surfaces of the workpiece model.

In order to consider a precautionary condition, the thermal memory of the previous cutting operations on the workpiece, namely the heat generated by tool 1 and tool 2 (see the Type A in Table 1) is also considered by assuming that tool 3 transfers the heat all along the first 7 hole partitions, despite its contact is only at the last one.

4.2. Results of FEM

The trial-and-error approach, aimed at the estimation of the maximum temperature developed on the two zones of the drilling tool, produced a value of 66 °C and 62 °C for the guided and free cutting conditions, respectively. These temperatures are the input for the transient simulations that compare the PU and the biological bone behaviors. The model validation results are reported in Table 3. In the guided condition case, both the temperature increment developed on the shank and the average temperature on the tool's body are matched.

The results of the numerical investigations on mandible models to predict the spatial distribution of the temperature are given in Fig. 23. The figure shows that although the temperature distribution in human bones covers a wider area compared to PU material, the basal temperature is reached in a very short distances (less than 3 mm in the case of bone with lower conductivity).

For further understanding, the temperature-drop in a location close to interface surface (0.5 mm from the internal hole surface), is investigated in time domain, Fig. 24. This provides information about the critical temperatures reached and how long the bone is affected from these temperatures. As can be seen in Fig. 24 a, the temperature drops very rapidly excluding the risk of thermal necrosis. It is reminded here that thermal osteonecrosis happens if a critical temperature (between 47 °C and 55 °C is maintained for at least a minute (Timon and Keady, 2019)). Considering that this simulated temperature profile refers to a point located near the tool-material interface, a worst-case scenario for the tissue damage is considered. It can be then concluded that even in case of surgery applied on human bone, the critical conditions for tissue damage do not occur by adopting the surgical guide operations.

Fig. 25 a shows the heat distribution on polyurethane and bone mandible models. On the other hand, Fig. 25 b shows how the heat distribution is constructed on human bone. In both figures, there is a section view of the jaw showing the distribution of heat in the plane the model. In the steady state simulations, the fixed heat source was used (of 66°) for 15 s.

5. Discussion

The conducted experimental campaign was performed at constant cutting parameters equal to the value suggested by the tool kit manufacturer. In one side, in a free cutting (without guiding mask) operation of bone drilling, the effect of cutting parameters on temperature rise is very strong as already demonstrated in the literature (Scarano et al., 2020), (Karaca et al., 2011). In particular, two critical parameters must

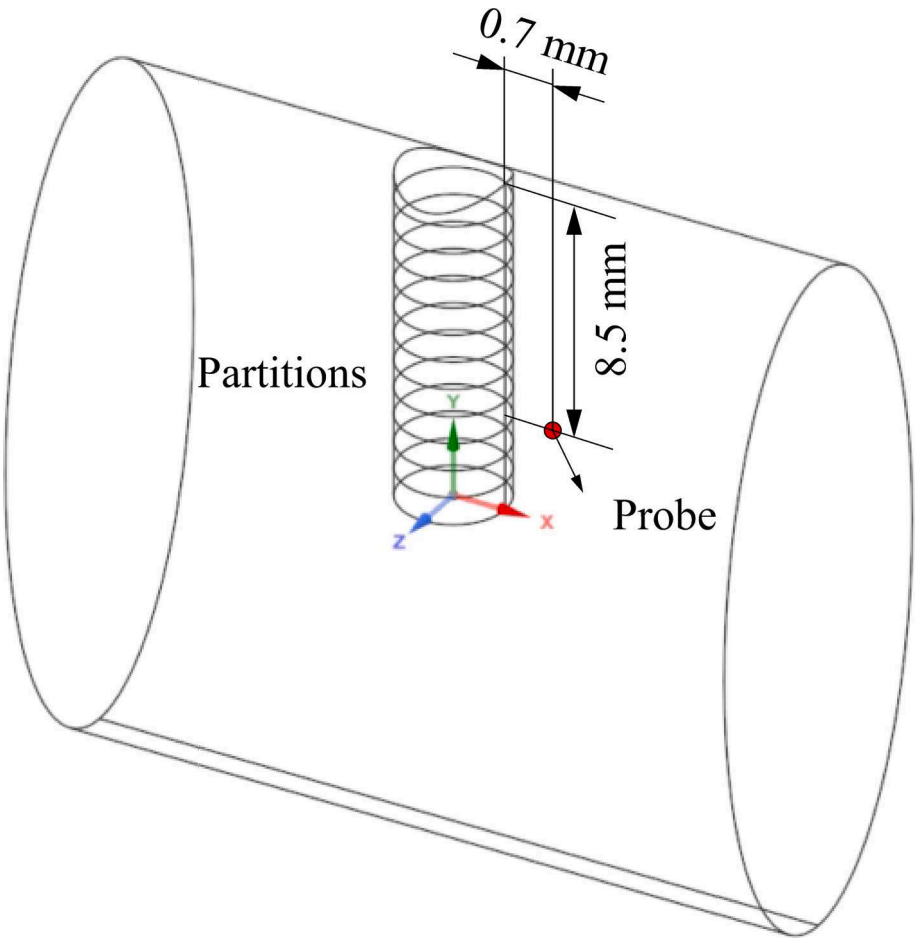

Fig. 22. Drilled hole partitions modelled in the FEM with the probing point where the temperature is read.

Table 3
Validation of the experimental and numerical analysis. For the zones definition refer to Fig. 21.

	Numerical		Experimental	
	Non-guided	Guided	Non-guided	Guided
T zone 1 [°C]	44 (average)	46.7 (average)	45.1 ± 1.87	46.4 ± 4.16
ΔT (zone 1 – zone 2 [°C])	3.6	4.6	2.6 (average)	4.6 (average)

be considered: the amount of generated heat during the cutting operation and the duration of the tissue's overheating (Davidson and James, 2003).

However, some of these parameters may have an additional effect on heat generation in guided drilling because they have a direct effect on the thermal power and energy dissipated by friction with the guide bushing. In particular, feed rate directly affects the cutting duration and MRR (the amount of chip removed in the unit of time) and with them the thermal power dissipated by the cut (Matthews and Hirsch, 1972), (Karaca et al., 2011), but it also affects the duration of the tool-guide contact and thus the thermal energy dissipated by the guide. Therefore, knowing if the overall effect of the feed value on the temperature reached by the tool in guided cutting operations is positive or negative required further investigations since this depends on how much the above two contributions weigh.

The other important parameter that has definite effect on the thermal power dissipated both due to cutting but also due to the presence of the guide is the tool rotational speed. Rotating the tool at higher speeds

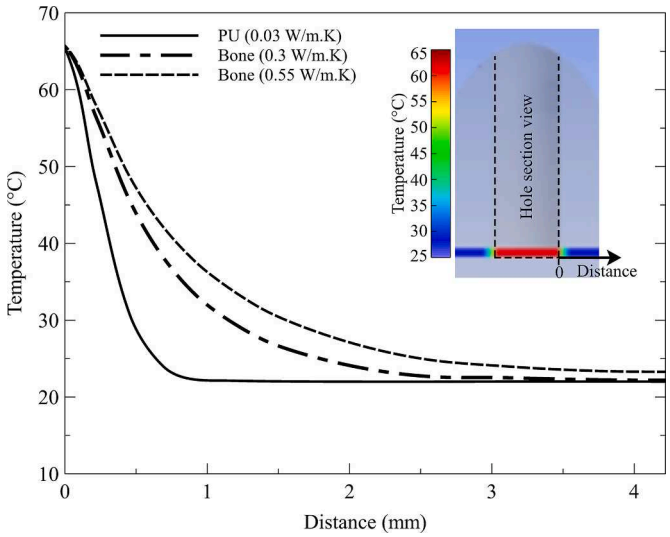

Fig. 23. Spatial distribution of temperature during guided surgery (tool-bone interface temperature equal to 66 °C) on polyurethane model (continuous line) and bone models with two different values of thermal conductivity (0.55 W/m•K: dashed line and 0.3 W/m•K dashed-dot line).

(which means higher tangential cutting speed reached at the tool tip) leads to an increase in the thermal power dissipated by the cut (Aldabagh, 2009) but also leads, without any margin of doubt, to greater thermal dissipation in the contact between tool shank and guide

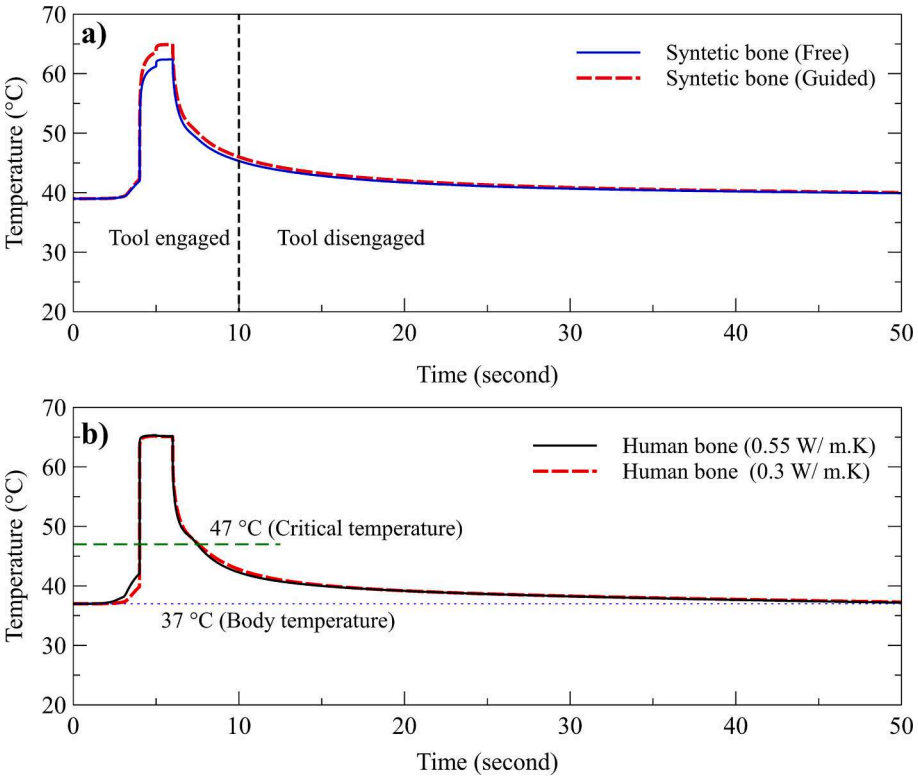

Fig. 24. Temperature drop in the polyurethane jaw model (a), and in the human bone (b) (sampled 0.5 mm away in radial distance at a depth of 8.5 mm from the top surface from the external hole surface with imposed 62 °C and 66 °C temperature for the free and guided condition, respectively), considering two different value of heat conductivity from literature (Davidson and James, 2000; Tissue Properties). The basal temperature in the bone simulations is set to 37 °C.

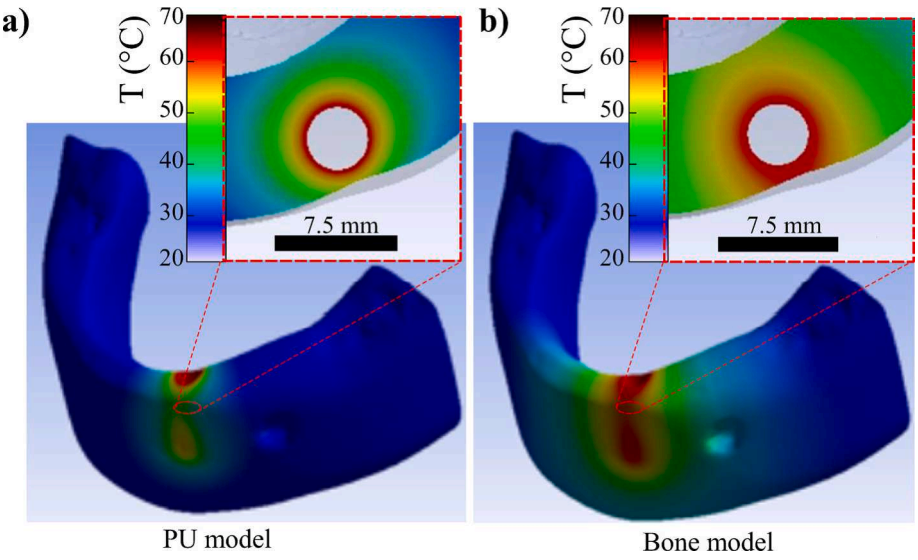

Fig. 25. Heat distribution on the jaws with fixed heat source with 66 °C for 15 s. PU model (a) and human bone model (b).

bushing.

The geometry of the guide bushing is the design element that needs to be controlled the most to manage the heat input dissipated due to the "guiding" friction. Keep in mind, that the length of the contact zone determines the useful drilling stroke of the tools (since during the entire axial stroke conducted the tools must remain in contact with the guide) but it also conditions the thermal power dissipated by friction and the stiffness of the entire coupling system. To ensure guided drilling accuracy a rigid coupling namely a high contact length and with a low clearance value, is needed. A large contact length results in a large contact area with a consequent effect on contact pressure and thus on heat dissipation (for the same contact force, pressure decreases with large areas, decreasing heat power dissipation). Obviously, the contact area is determined by the diameter of the contact area which is therefore a key variable to be managed at the design stage. However, the diameter has another important dynamic effect on temperature since it conditions the tangential speed of contact between tool and bushing, which has a direct effect on the thermal power dissipated by friction and eventually on the wear resistance of the contact areas (this aspect is less relevant with Type A integrated bushing since guides are patient-specific and

mostly single-use, but it can be more important with external adapters as Type B). It is also true that the contact pressure between shank and bushing is the other variable that determines the increase in frictional power dissipated but this depends on the cutting process and the local characteristics of the cut bone, factors that cannot be subject to design. In the experiments, Type A and Type B tools have shanks with different diameters in contact but also different rotational speeds at which they are used (however, the shank contact speeds in the two cases were similar).

In our study, we tested how two different geometries of guided drilling tool kits behave with the aim of understanding whether the template leads to temperature rise in a variety of situations. Thus, the purpose was not to directly compare the two solutions but was to find whether the template leads to temperature rise. Given, however, the whole effects that tool geometries have on temperature rise (Lee et al., 2011), (Augustin et al., 2008), the most correct technological comparison should have been made by comparing the temperature rise in guided surgery tools (with their specific geometry) with the temperature rise in free surgery tools (with their specific geometry). From a methodological and scientific point of view, however, this would have meant having guided and free tool kits with perfectly equal cutting geometry and materials, which was not possible to have.

In the experiments, the temperature generated on the tool shank due to friction with the guide was found to be lower than the temperature that reached the cutting edge areas of the tool, and this leads to say that for the tools tested, the cutting effect is the main one for their temperature increase. This result depends both on the amount of heat input that the two effects introduce into the system but also on the thermal capabilities of the tools and their mass distribution. Therefore, this result is strictly dependent on the geometry of the tools tested. This places a limitation on the generalizability of the results obtained on other tool geometries than those under study.

Furthermore, along this line of reasoning, it was pointed out that during guided drilling the tools show a temperature distribution that is much more homogeneous along the axial coordinate while during free cutting tests the tool is shown to be heated up only in the vicinity of the cutting tip and helix. This effect highlights the fact that the overall length of the drilling tool is also a magnitude that conditions the tendency of the thermal disturbance produced by the tool shank in contact with the guide to reach the areas of the cut. Long tools, therefore, are certainly less likely to carry the thermal disturbance from the guided shank toward the critical areas in contact with the bone. This may suggest the adoption of particular incremental drilling strategies (i.e., a particular sequence of tools to achieve the design depth and diameter of the holes for the dental implants) in the various guided drilling kits.

Both types of tools used have a flange in guided surgery tools that is responsible for stopping their axial travel (this is the axial limit stop). It has been shown that this geometric element overheats more than the other areas of the tool both due to its larger diameter (and therefore higher contact speed) but mainly due to the axial contact pressure achieved. In the tools tested, the heat dissipation generated in this circular ring appears to be unable to propagate to the cutting zone of the tool. In any case, limiting the dwelling steps at the end of the drilling process and limiting the axial thrust force when the tool reaches the lower coordinate is a strategy that surgerists might want to adopt to limit this effect.

The temperature rise data in guided drilling show, compared to free drilling, a greater variability that we traced back to the variability of the contact pressure that the tool exerts on the guide bushing. This variability is related, in our opinion, to the evolutionary mechanism of the cutting process whereby the tool penetrates the material according to a direction (i.e., the axis of the hole) that varies slightly from condition to condition, depending on the local bone density, clearance and flexibility in the tool holder. This mechanism is intrinsic to the positioning action of the template, which is manifested precisely by the X/Y force on the plane. The action of the guide is decisive in the initial stages of drilling but as the tool penetrates in “deep” holes, the axis of the hole tends to be misaligned thus creating more shank contact pressure on the bushings. In other words, the pressure on the guide bushing (and thus the heat generated) is a function of how far the tool can penetrate the bone aligned with respect to the bushing. This variable component in our opinion is unpredictable.

Type A tools used in dry condition show a relevant absolute temperature increase, but the contribution related to the presence of the guide is much less relevant (namely there is less different between the guided and free condition), indicating therefore that in dry cutting the major contribution of heat generated is related to material removal and not to guide friction or other thermal dissipation issues caused by the guide. With Type B instead, the water makes all the difference. It cools everything down and everything is kept cold. Interestingly, however, the quantified thermal effect of the guide resulted greater.

The aqueous solution used as cooling liquid allows the heat produced to be cooled, but also allows less heat to be produced as it reduces the friction between the relative moving parts (Lee et al., 2011). So, the cutting process certainly benefits from the presence of water as the friction coefficient between bone and tool is reduced, and the cutting area is kept clean. The friction between tool shank and bushing in the guide template could also benefit from the presence of water but only if water reaches the sliding zones, which is not trivial. Instead, the use of dry cutting, coupled with the use of high-performance anti-friction coatings as the one adopted in Type A has the added value of simplifying surgical operations and solution setup.

There could be also some additional difference in Type A and Type B solution related to the internal versus external adapter. The integrated Type A bushing is more convenient and easier to use but can creates the risk that thermal expansion will cause the bushing to be pulled out in the housing while with the external adapter solution this risk is not there.

The FEM model in this study was developed with the precise aim of translating the results obtained on synthetic bone into the biological bone case. Therefore, the adopted model was simplified from the drilling thermal generation point of view. It in fact considers the heat generation caused by the drilling a steady-state generation that is happening only at the tool-tip. This simplification is usually adopted in literature even in more complex models as the one presented in (Davidson and James, 2003). Therefore, there are aspects that have been neglected as the significant effects of moving chips, specific aspects that governs the heat transfer between the drill bit and the bone and heat convection from the drill bit to the surroundings outside the bone. The use of FEM however can give better insights in terms of geometrical dissipation of the heat with respect to other modelling techniques, as the analytical methods provided in (Kalidindi, 2004) since they allow more easily to take into account complex geometries with its related boundary conditions. There are situations however where the ordinary heat diffusion equations for the bone material and the heat generation at the drill tip, arising from the cutting process and friction can be integrated in much more complex models, as the one presented in (Lee et al., 2011) that allows parametric studies to be conducted on the effect of the various parameters involved.

Despite being simplified, the finite element model developed in this work, was successful in proving a clear picture of what happens on biological bone with respect to synthetic ones and providing insight on the geometrical effects. It was in fact highlighted that hole location plays a key role on heat conduction/dissipation within the bone. Especially, when the holes are positioned on the areas of low thickness (such as the front of the jaw) the heat transfer by conduction is greatly affected by the position since the effects of boundaries (related to the fact that by convection the heat is transferred less effectively) weigh heavily. In this sense, the jaw has an additional thermal effect that can be assumed as indirect since it is related to the greater hole placement capabilities that it provides compared to the traditional solution.

6. Conclusions

This study reveals that the presence of the dental surgical guide systematically increases the tool temperature compared to non-guided case. The conducted experiments on Polyurethane synthetic bone show on one side that these temperature effects depend on the adopted guiding and tooling system, by the presence of the refrigerant fluid, and by the specific planar forces developed during the drilling operation. On the other hand, the study reveals that the magnitude of the introduced thermal effect is generally quite low, being quantified in average of +4/5 °C, between the guided and the free surgery. Finite element models indicate that this minimal impact is not harmful to biological tissues and therefore no special actions should be taken in addition to the standard drilling procedures suggestions prescribed by the dental tooling kit suppliers. Future experiments on human bones or in-vivo with IR thermal sensing may further validate findings in the presence of natural variability sources such as patient-specific bone characteristics, blood, soft tissues, and manual surgery operations.

CRediT authorship contribution statement

Francesca Pupulin: Writing – original draft, Validation, Software, Methodology, Investigation, Formal analysis, Data curation. **Giorgio Oresta:** Writing – original draft, Visualization, Validation, Software, Methodology, Formal analysis, Data curation. **Talha Sunar:** Writing – review & editing, Visualization, Validation, Supervision, Software, Investigation, Formal analysis, Data curation. **Paolo Parenti:** Writing – review & editing, Writing – original draft, Validation, Supervision, Resources, Project administration, Methodology, Investigation, Funding acquisition, Conceptualization.

Declaration of competing interest

The authors declare that they have no known competing financial interests or personal relationships that could have appeared to influence the work reported in this paper.

Data availability

Data will be made available on request.

Acknowledgements

The authors acknowledge Eng. Tarachand, Eng. Dassi, Dott. Carini, Dr. Malguzzi from MULTYSYSTEM for their active support to the present work.

Appendix. Material properties

Table 4
Nominal material properties of the adopted surgical guides

Dental resins		
	Type A (Formlabs Dental Resin)	Type B (Stratasys Dental Materials)
Tensile strength	73 MPa	50-65 MPa
Elongation at break	12%	15-25 %
Modulus of elasticity	2900 MPa	2300-3300 MPa
Flexural strength	>102 MPa	75-110 MPa
Flexural modulus	2500 MPa	2300-3200 MPa
Hardness	67 D (Shore)	73-76 (Scale M)
Polymerized density	/	1170-1180 kg/m^3
Bio-compatibility	class I, ISO approved	ISO approved

References

Aldabagh, A.H., 2009. The significance of motor speed on heat generation during implant drilling (experimental study on bovine bone). Al-Rafidain Dent. J. 9, 303–306. https://doi.org/10.33899/rden.2009.9121.

ASTM F1839 - 97: standard specification for rigid polyurethane foam for use as a standard material for testing orthopaedic devices and instruments. ASTM B. Stand. 13.01, 2014, 6–11.

ASTM F1839 - 08, 2012. Standard Specification for Rigid Polyurethane Foam for Use as a Standard Material for Testing Orthopaedic Devices and Instruments. ASTM B. Stand.

Augustin, G., Davila, S., Mihoci, K., Udiljak, T., Vedrina, D.S., Antabak, A., 2008. Thermal osteonecrosis and bone drilling parameters revisited. Arch. Orthop. Trauma Surg. 128, 71–77. https://doi.org/10.1007/s00402-007-0427-3.

Bai, W., Pan, P., Shu, L., Yang, Y., Zhang, J., Xu, J., Sugita, N., 2021. Design of a self-centring drill bit for orthopaedic surgery: a systematic comparison of the drilling performance. J. Mech. Behav. Biomed. Mater. 123, 104727 https://doi.org/10.1016/j.jmbbm.2021.104727.

Bien-air dental *IChiropro surgery*. website. https://dental.bienair.com/en_us/products/oral-surgery-implantology.html. January 2023.

Calvert, K.L., Trumble, K.P., Webster, T.J., Kirkpatrick, L.A., 2010. Characterization of commercial rigid polyurethane foams used as bone analogs for implant testing. J. Mater. Sci. Mater. Med. 21, 1453–1461. https://doi.org/10.1007/s10856-010-4024-6.

Chen, R., Chang, R.C., Tai, B., Huang, Y., Ozdoganlar, B., Li, W., Shih, A., 2020. Biomedical manufacturing: a review of the emerging research and applications. J. Manuf. Sci. Eng. Trans. ASME 142, 1–24. https://doi.org/10.1115/1.4048043.

Choi, Y.S., Oh, J.W., Lee, Y., Lee, D.W., 2022. Thermal changes during implant site preparation with a digital surgical guide and slot design drill: an ex vivo study using a bovine rib model. J. Periodontal Implant Sci. 52, 411–421. https://doi.org/10.5051/jpis.2106040302.

Davidson, S.R.H., James, D.F., 2000. Measurement of thermal conductivity of bovine cortical bone. Med. Eng. Phys. 22, 741–747. https://doi.org/10.1016/S1350-4533(01)00003-0.

Davidson, S.R.H., James, D.F., 2003. Drilling in bone: modeling heat generation and temperature distribution. J. Biomech. Eng. 125, 305–314. https://doi.org/10.1115/1.1535190.

Fernandes, M.G.A., Fonseca, E.M.M., Natal, R.J., 2016. Thermal analysis during bone drilling using rigid polyurethane foams: numerical and experimental methodologies. J. Brazilian Soc. Mech. Sci. Eng. 38, 1855–1863. https://doi.org/10.1007/s40430-016-0560-4.

Formlabs dental resin - surgical guide. website. https://dental.formlabs.com/it/. January 2023.

Frösch, L., Mukaddam, K., Filippi, A., Zitzmann, N.U., Kühl, S., 2019. Comparison of heat generation between guided and conventional implant surgery for single and sequential drilling protocols—an in vitro study. Clin. Oral Implants Res. 30, 121–130. https://doi.org/10.1111/clr.13398.

Kalidindi, V., 2004. UKnowledge OPTIMIZATION of DRILL DESIGN and. COOLANT SYSTEMS.

Karaca, F., Aksakal, B., Kom, M., 2011. Influence of orthopaedic drilling parameters on temperature and histopathology of bovine tibia: an in vitro study. Med. Eng. Phys. 33, 1221–1227. https://doi.org/10.1016/j.medengphy.2011.05.013.

Lee, J.E., Rabin, Y., Ozdoganlar, O.B., 2011. A new thermal model for bone drilling with applications to orthopaedic surgery. Med. Eng. Phys. 33, 1234–1244. https://doi.org/10.1016/j.medengphy.2011.05.014.

Matthews, L., Hirsch, C., 1972. Temperatures Measured in Human Cortical Bone when Drilling.

Migliorati, M., Amorfini, L., Signori, A., Barberis, F., Silvestrini Biavati, A., Benedicenti, S., 2013. Internal bone temperature change during guided surgery preparations for dental implants: an in vitro study. Int. J. Oral Maxillofac. Implants 28, 1464–1469. https://doi.org/10.11607/jomi.2854.

Misch, C.E., 2007. Contemporary Implant Dentistry. Elsevier.

Misir, A.F., Sumer, M., Yenisey, M., Ergioglu, E., 2009. Effect of surgical drill guide on heat generated from implant drilling. J. Oral Maxillofac. Surg. 67, 2663–2668. https://doi.org/10.1016/j.joms.2009.07.056.

Ruga, E., Amerio, E., Carbone, V., Volante, M., Gandolfo, S., 2017. Physics and histologic evaluation of rotary, ultrasonic, and sonic instruments. J. Craniofac. Surg. 28, e609–e614. https://doi.org/10.1097/SCS.0000000000003738.

Scarano, A., Lorusso, F., Noumbissi, S., 2020. Infrared thermographic evaluation of temperature modifications induced during implant site preparation with steel vs. Zirconia implant drill. J. Clin. Med. 9 https://doi.org/10.3390/jcm9010148.

Stocchero, M., Jinno, Y., Toia, M., Ahmad, M., Papia, E., Yamaguchi, S., Becktor, J.P., 2019. Intraosseous temperature change during installation of dental implants with two different surfaces and different drilling protocols: an in vivo study in sheep. J. Clin. Med. 8, 1198. https://doi.org/10.3390/jcm8081198.

Stocchero, M., Sivolella, S., Brunello, G., Zoppello, A., Cavallin, F., Biasetto, L., 2021. Bone temperature variation using a surgical 3d-printed surgical guide with internal irrigation. Appl. Sci. 11. https://doi.org/10.3390/app11062588.

Stratasys dental materials. website. https://www.stratasys.com/it/materials/materials-catalog/polyjet-materials/dental-materials. January 2023.

Sugita, N., Osa, T., Mitsuishi, M., 2009. Analysis and estimation of cutting-temperature distribution during end milling in relation to orthopedic surgery. Med. Eng. Phys. 31, 101–107. https://doi.org/10.1016/j.medengphy.2008.05.001.

Sui, J., Sugita, N., Mitsuishi, M., 2015. Thermal modeling of temperature rise for bone drilling with experimental validation. J. Manuf. Sci. Eng. Trans. ASME 137, 1–10. https://doi.org/10.1115/1.4030880.

Szivek, J.A., Thomas, M., Benjamin, J.B., 1993. Characterization of a synthetic foam as a model for human cancellous bone. J. Appl. Biomater. 4, 269–272. https://doi.org/10.1002/jab.770040309.

Tatakis, D.N., Chien, H.H., Parashis, A.O., 2000. Guided implant surgery risks and their prevention. Periodontol 81, 194–208. https://doi.org/10.1111/prd.12292, 2019.

Thompson, M.S., McCarthy, I.D., Lidgren, L., Ryd, L., 2003. Compressive and shear properties of commercially available polyurethane foams. J. Biomech. Eng. 125, 732–734. https://doi.org/10.1115/1.1614820.

Timon, C., Keady, C., 2019. Thermal osteonecrosis caused by bone drilling in orthopedic surgery: a literature review. Cureus. https://doi.org/10.7759/cureus.5226.

Tissue Properties. Foundation for research on information technologies in society (IT'IS). website: https://itis.swiss/virtual-population/tissue-properties/database/heat-generation-rate/. January 2023.

Türker, H., Aksoy, B., Özsoy, K., 2022. Fabrication of customized dental guide by stereolithography method and evaluation of dimensional accuracy with artificial neural networks. J. Mech. Behav. Biomed. Mater. 126. https://doi.org/10.1016/j.jmbbm.2021.105071.

Waltenberger, L., Wied, S., Wolfart, S., Tuna, T., 2022. Effect of different dental implant drilling template designs on heat generation during osteotomy – an in vitro study. Clin. Oral Implants Res. 33, 53–64. https://doi.org/10.1111/clr.13864.